



August 2004

A Semi-Implicit Time-Stepping Model For Frictional Compliant Contact Problems

Peng Song
University of Pennsylvania

Jong-Shi Pang
Johns Hopkins University

R. Vijay Kumar
University of Pennsylvania, kumar@grasp.upenn.edu

Follow this and additional works at: https://repository.upenn.edu/meam_papers

Recommended Citation

Song, Peng; Pang, Jong-Shi; and Kumar, R. Vijay, "A Semi-Implicit Time-Stepping Model For Frictional Compliant Contact Problems" (2004). *Departmental Papers (MEAM)*. 47.

https://repository.upenn.edu/meam_papers/47

Postprint version. "This is a preprint of an article published in *International Journal for Numerical Methods in Engineering*, Volume 60, Issue 13, 7 August 2004, pages 2231-2261."

Publisher URL: <http://dx.doi.org/10.1002/nme.1049>

This paper is posted at ScholarlyCommons. https://repository.upenn.edu/meam_papers/47
For more information, please contact repository@pobox.upenn.edu.

A Semi-Implicit Time-Stepping Model For Frictional Compliant Contact Problems

Abstract

In this paper, we formulate a semi-implicit time-stepping model for multibody mechanical systems with frictional, distributed compliant contacts. Employing a polyhedral pyramid model for the friction law and a distributed, linear, viscoelastic model for the contact, we obtain mixed linear complementarity formulations for the discrete-time, compliant contact problem. We establish the existence and finite multiplicity of solutions, demonstrating that such solutions can be computed by Lemke's algorithm. In addition, we obtain limiting results of the model as the contact stiffness tends to infinity. The limit analysis elucidates the convergence of the dynamic models with compliance to the corresponding dynamic models with rigid contacts within the computational time-stepping framework. Finally, we report numerical simulation results with an example of a planar mechanical system with a frictional contact that is modeled using a distributed, linear viscoelastic model and Coulomb's frictional law, verifying empirically that the solution trajectories converge to those obtained by the more traditional rigid-body dynamic model.

Comments

Postprint version. "This is a preprint of an article published in *International Journal for Numerical Methods in Engineering*, Volume 60, Issue 13, 7 August 2004, pages 2231-2261."

Publisher URL: <http://dx.doi.org/10.1002/nme.1049>

A Semi-Implicit Time-Stepping Model For Frictional Compliant Contact Problems*

Peng Song[†], Jong-Shi Pang[‡] and Vijay Kumar[§]

May 6, 2003

Abstract

In this paper, we formulate a semi-implicit time-stepping model for multibody mechanical systems with frictional, distributed compliant contacts. Employing a polyhedral pyramid model for the friction law and a distributed, linear, viscoelastic model for the contact, we obtain mixed linear complementarity formulations for the discrete-time, compliant contact problem. We establish the existence and finite multiplicity of solutions, demonstrating that such solutions can be computed by Lemke's algorithm. In addition, we obtain limiting results of the model as the contact stiffness tends to infinity. The limit analysis elucidates the convergence of the dynamic models with compliance to the corresponding dynamic models with rigid contacts within the computational time-stepping framework. Finally, we report numerical simulation results with an example of a planar mechanical system with a frictional contact that is modeled using a distributed, linear viscoelastic model and Coulomb's frictional law, verifying empirically that the solution trajectories converge to those obtained by the more traditional rigid-body dynamic model.

1 Introduction

This paper addresses the dynamic simulation of mechanical systems with frictional compliant contacts. Constraints that arise in systems with contact are called unilateral constraints because the contact forces and the relative separation and slip between rigid objects can be defined so that they are always nonnegative [24]. Excellent reviews of the state-of-the-art in rigid-body dynamic simulation with unilateral constraints can be found in [9, 36].

The use of Coulomb's friction law with the principles of classical rigid-body dynamics introduces mathematical inconsistencies. Specifically, in a forward dynamics problem, if all contacts

*This work is based on research supported by the National Science Foundation under a Focused Research Group Grant DMS-0139715.

[†]Department of Mechanical Engineering and Applied Mechanics, University of Pennsylvania, Philadelphia 19104-6391, U.S.A. Email: pengs@grasp.cis.upenn.edu.

[‡]Corresponding author. Department of Mathematical Sciences, The Johns Hopkins University, Baltimore, Maryland 21218-2682, U.S.A. Email: pang@mts.jhu.edu. The work of this author is partly supported by the National Science Foundation under grant CCR-0098013.

[§]Department of Mechanical Engineering and Applied Mechanics, University of Pennsylvania, Philadelphia 19104-6391, U.S.A. Email: kumar@grasp.cis.upenn.edu.

are known to be rolling (sticking), the existence of a solution for the accelerations can be shown if the constraints are linearly independent [38]. In all other cases, the initial value problem can have no solution or multiple solutions for special choices of initial conditions [24, 42]. These difficulties can be traced back to two distinct aspects of the model. First, when the number of contact forces (normal and tangential) is greater than three in planar systems (six in spatial systems), the system is statically indeterminate and the contact forces cannot be uniquely determined. As a result, it is difficult to incorporate any frictional model that relates normal and tangential forces to relative velocities. Second, in models of dry friction [5], frictional forces (and moments) depend in a nonsmooth fashion on reaction forces and relative velocities, which in turn are functions of accelerations. The nonsmooth nature of this dependence leads to difficulties with proofs of existence and uniqueness.

One approach to overcoming these difficulties is by using an explicit model of the compliance at contacts between nominally rigid bodies. In a *compliant contact model*, constitutive laws are used to relate contact forces with local deformations [15, 34, 43]. The simplest example of such models can be found in penalty-function methods [1, 44], in simulation of soft tissue [22] and physics-based simulation in graphics [20]. In these papers, compliance is used to prescribe normal contact forces as a function of normal displacements. The model considered here is phenomenologically more correct. In addition to normal compliance, it incorporates tangential compliance, coupling friction with local deformations in a fundamental way. Continuum models for modeling the deformations at each contact are described in [16, 32, 41, 43]. Existence and uniqueness can be shown for continuum models provided the maximum tangential force at each point is *a priori* known [16]. Alternatively, lumped models of compliance that capture linear viscoelastic behavior are used in [15, 34]. Proofs of existence and uniqueness along with a singular perturbation analysis for a single-contact planar system are provided in [34]. For such a system, the solution is shown to converge to the traditional rigid-body dynamic model in the limit of zero compliance.

The forward dynamics problem for mechanical systems with frictional contacts was first formulated as a *Linear Complementarity Problem* (LCP) by Lötstedt [24]. Lötstedt also gives existence and uniqueness conditions for a planar system. These conditions were further generalized by Baraff [6]. Once the problem is formulated as an LCP, the existence and uniqueness conditions can be derived from LCP theory; see [12] for a comprehensive treatment of the LCP. Extensive results on LCP formulations for rigid-body dynamics with Coulomb frictional contacts can be found in [30, 38]. It is shown that the existence and uniqueness of rigid-body solutions can be guaranteed for three-dimensional systems if the coefficients of friction at both rolling and sliding contacts are below an upper bound. But it is difficult, in practice, to obtain an analytical expression for such an upper bound. Our work extends the rigid-body results to mechanical systems with compliant frictional contact.

The approach we take in this paper is influenced by the extensive recent work on *time-stepping methods* for dynamic simulation of rigid-body systems in frictional contact [2, 3, 4, 35, 36, 37, 39]. Instead of developing integrators that numerically solve continuous equations of motion while respecting the constraints on the state variables, time-stepping methods directly discretize the equations of motion and the associated constraints automatically, thus guaranteeing the satisfaction of the constraints. We will show the existence of solutions for time-stepping compliant contact models, and demonstrate the convergence of these solutions to solutions ob-

tained by rigid body dynamic models (when these are available) as the contact compliance is reduced to zero.

The modeling in the paper is an extension of the first author’s Ph.D. thesis [33] in which each contact was modeled by a nonlinear but decoupled springs and dampers in the normal and tangential direction. In contrast, in this work, each contact is modeled as a finite patch (as opposed to a point contact) and constitutive laws derived from linear viscoelastic theory are used to relate small normal and tangential deformations to the distribution of stresses in the contact patch. In so doing, we ignore the effect of the inertia associated with deformations. An important advantage of this approach is the ability to model more sophisticated aspects of frictional contacts by allowing for smooth transitions between contact and separation, and between stick and slip at each point in the contact patch. Thus it incorporates microslip [28] and can be easily extended to model local adhesion, asperities, and nonlinear, nonlocal frictional laws [19, 28].

We do not explicitly consider frictional impacts, another important and relevant area in dynamic simulation. Goyal [15] and Kraus [21] derive models for frictional impacts from compliance models as alternatives to rigid body impact models developed by Brach [8], Chatterjee and Ruina [11], and Mirtich [27]. Marghitu and Hurmuzlu employ continuum models for the study of frictional impacts [26]. While the model and the solution methodology proposed in this paper lends themselves to solving problems with frictional impacts, our goal, in this paper, is to focus on problems with finite force solutions.

The paper is organized as follows. In the next section, we derive a time-stepping framework for dynamic simulation of systems with distributed compliance. We show that the discrete-time, distributed compliant model can be formulated as mixed complementarity problems. In Section 4, we establish the conditions for existence and finite multiplicity of solutions based on the complementarity problem formulation. In Section 5, we undertake a limit analysis within the time-stepping framework and prove that the solution to the distributed compliant model converges to that of the corresponding rigid-body models. Numerical implementation and results are presented in Section 6.

2 Time-Stepping Models

We present in this section the semi-implicit time-stepping, frictional compliant contact model that is the main object of study in this paper. There are three major components of such a model: the dynamic equations of motion, the distributed compliant model, and the frictional contact conditions. These are described in three different subsections.

2.1 Equations of motion

The dynamic equation of motion for a multibody system with frictional contacts can be written in the form

$$M(q)\dot{\nu} = f(t, q, \nu) + G(q)^T [J\Psi_n(q)^T \lambda_n + J\Psi_t(q)^T \lambda_t + J\Psi_o(q)^T \lambda_o], \quad (1)$$

where q is the n_q -dimensional vector of generalized coordinates, ν is the n_ν -dimensional vector of the system velocities. $M(q)$ is the $n_\nu \times n_\nu$ symmetric positive definite inertia matrix, $f(t, q, \nu)$

is the n_ν -dimensional external force vector (excluding contact forces), $G(q)$ is a $n_q \times n_\nu$ Jacobian matrix¹, $\lambda_{n,t,o}$ are the contact force vectors in the normal direction (labelled n) and the two tangential directions (labelled t and o) and $J\Psi_{n,t,o}(q)$ are the Jacobian matrices corresponding to the contact forces. For rigid-body systems, $\lambda_{n,t,o}$ are n_c -dimensional vectors, and $J\Psi_{n,t,o}(q)$ are $n_c \times n_q$ matrices, where n_c is the total number of contacts. For compliant contact models, the dimensions of these forces and Jacobians are related to the compliance model being used — see Subsection 2.2 for details. The kinematics equations relate the system velocity ν to the time-derivative of the system configuration $\dot{q} \equiv dq/dt$ via the parametrization matrix $G(q)$:

$$\dot{q} = G(q)\nu. \quad (2)$$

Together, (1) and (2) constitute the equations of motion given by the dynamics of the mechanical system.

We consider a time discretization of the differential equations (1) and (2) for $t \in (0, T]$. Fix a positive integer N and let $h \equiv T/N$. Partition the interval $[0, T]$ into N subintervals $[t_\ell, t_{\ell+1}]$, where $t_\ell \equiv \ell h$, for $\ell = 0, 1, \dots, N$. Write

$$q^\ell \equiv q(t_\ell), \quad \nu^\ell \equiv \nu(t_\ell), \quad \text{and} \quad \lambda_{n,t,o}^\ell \equiv \lambda_{n,t,o}(t_\ell).$$

The time derivatives $\dot{\nu}$ and \dot{q} are replaced by the backward Euler approximations: for all $\ell = 0, \dots, N-1$,

$$\dot{\nu}(t_{\ell+1}) \approx \frac{\nu^{\ell+1} - \nu^\ell}{h} \quad \text{and} \quad \dot{q}(t_{\ell+1}) \approx \frac{q^{\ell+1} - q^\ell}{h}.$$

The various time-stepping schemes differ in how $M(q)$ and the right-hand sides in (1) and (2) are approximated. In the *fully implicit scheme*, which is the version employed in the recent doctoral thesis [40] for the numerical simulation of multi-rigid-body systems with frictional contact, all functions are evaluated at time $\ell+1$, resulting in the following nonlinear algebraic equation:

$$M(q^{\ell+1})(\nu^{\ell+1} - \nu^\ell) = h f(t_{\ell+1}, q^{\ell+1}, \nu^{\ell+1}) + G(q^{\ell+1})^T \left[J\Psi_n(q^{\ell+1})^T \lambda_n^{\ell+1} + J\Psi_t(q^{\ell+1})^T \lambda_t^{\ell+1} + J\Psi_o(q^{\ell+1})^T \lambda_o^{\ell+1} \right].$$

Because the inertia matrix and the Jacobians are functions of $q^{\ell+1}$, solving for the unknown $q^{\ell+1}$ involves the solution of nonlinear equations. In contrast to the fully implicit scheme, a *semi-implicit* scheme is a modification that results in a linear problem formulation. Specifically, a semi-implicit discretization of (1) gives us:

$$M(q^\ell)(\nu^{\ell+1} - \nu^\ell) = h f(t_\ell, q^\ell, \nu^\ell) + G(q^\ell)^T \left[J\Psi_n(q^\ell)^T \lambda_n^{\ell+1} + J\Psi_t(q^\ell)^T \lambda_t^{\ell+1} + J\Psi_o(q^\ell)^T \lambda_o^{\ell+1} \right]. \quad (3)$$

Similarly, a semi-implicit discretization of (2) results in

$$q^{\ell+1} - q^\ell = h G(q^\ell) \nu^{\ell+1}. \quad (4)$$

¹The matrix $G(q)$ allows us to use different parameterizations for $SO(3)$, and to use speeds (ν) that are different from the derivatives of the coordinates.

The semi-implicit discretization scheme allows us to apply linear complementarity theory [12]². As we will show next, the compliant contact model and the frictional contact constraints can also be written in a semi-implicit form leading to a consistent problem formulation.

2.2 Distributed compliant contact model

The distributed compliant model relates the contact forces with the local deformations. At any contact point $v = 1, \dots, n_c$, we divide the patch that encloses the contact area into $n_s \times n_s$ small discrete elements with lumped stiffness and damping properties as depicted in Figure 1. In the 3-dimensional setting, each element has 3 sets of lumped spring-damper units, one for each of the n, t, and o directions. Further, we will require that the contact patches (contact points in the limiting case of rigid bodies) be distinct and non-overlapping. We will assume that the deformations at a contact patch are related to forces at that contact patch. In other words the local deformations at a particular contact point or contact patch are not directly affected by the forces at other contact patches. This is equivalent to saying that all deformations occur over a finite number of non-overlapping contact patches. At each contact patch v , we can write

$$\lambda^v = \mathcal{G}^v(\delta^v, \dot{\delta}^v), \quad (5)$$

where \mathcal{G}^v is a smooth function representing the mechanics of the contact patch v , δ^v is the vector of body deformations, and $\dot{\delta}^v$ is the vector of deformation rates.

In this paper, we make two assumptions about the form of \mathcal{G} . First, we assume that the contacting objects are viscoelastic and linear. Second, we assume the contacts are counterformal, an assumption that is common in contact mechanics and in robotics [14, 16, 18, 31]. The magnitude of the deformations and the size of the contact patch are functions of the material properties of the contacting objects and to some extent, the relative curvature of the contacting surfaces. The counterformal assumption means that both these magnitudes are small compared to the relative curvature of the contacting surfaces. Then, at each contact patch v , we have

$$\lambda^v = K^v \delta^v + C^v \dot{\delta}^v, \quad (6)$$

with

$$\lambda^v = \begin{pmatrix} \lambda_n^v \\ \lambda_t^v \\ \lambda_o^v \end{pmatrix} \in \mathfrak{R}^{3n_s^2}, \quad \delta = \begin{pmatrix} \delta_n^v \\ \delta_t^v \\ \delta_o^v \end{pmatrix} \in \mathfrak{R}^{3n_s^2},$$

and

$$K^v \equiv \begin{bmatrix} K_{nn}^v & K_{nt}^v & K_{no}^v \\ K_{tn}^v & K_{tt}^v & K_{to}^v \\ K_{on}^v & K_{ot}^v & K_{oo}^v \end{bmatrix}, \quad C^v \equiv \begin{bmatrix} C_{nn}^v & C_{nt}^v & C_{no}^v \\ C_{tn}^v & C_{tt}^v & C_{to}^v \\ C_{on}^v & C_{ot}^v & C_{oo}^v \end{bmatrix}.$$

²Although analysis of the the fully-implicit scheme is possible (using nonlinear complementarity theory similar to [29] and computational methods similar to those for rigid-body models [40]), the nonlinearity represents an additional level of complexity.

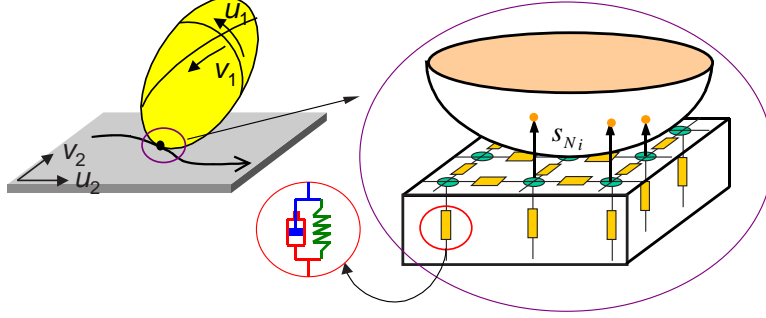


Figure 1: Distributed compliant model with coupled spring-damper elements.

The entries of the two symmetric matrices K^v and C^v are filled by influence functions that represent stiffness and damping properties, respectively³. For example, at the given contact patch v , $(K_{nn}^v)_{ij}$ (with $i, j = 1, \dots, n_s^2$) is the normal force that must be exerted at the i th element to produce a unit normal deformation at the j th element (and a zero deformation and a zero rate of deformation at any other element in the contact patch). Similarly, $(C_{tn}^v)_{ij}$ represents the tangential force in the tangential direction t at the i th element that is required to produce a unit change of deformation in the normal direction at the j th element (with a zero effect elsewhere). The stiffness matrix K^v is positive definite, since $\frac{1}{2}(\delta^v)^T K^v \delta^v$ is the potential energy stored in the system. The same argument holds for the damping matrix C , since $\frac{1}{2}(\dot{\delta}^v)^T C^v (\dot{\delta}^v)$ is the energy dissipation corresponding to any vector of possible deformation rates $\dot{\delta}^v$. While expressions for the damping matrix C are harder to obtain, it is common to assume [7] that K^v and C^v have a similar underlying structure. We will choose $C^v = 2\sqrt{K^v}$ to construct a critically damped system. If the material properties are nonlinear or if analytical expressions for the influence functions are not available, it is possible to obtain the influence functions using nonlinear finite element models with Rayleigh damping [7].

For a multibody system with n_c contacts, the system force variables $\lambda_{n,t,o}$, body deformations $\delta_{n,t,o}$, and deformation rates $\dot{\delta}_{n,t,o}$ are concatenations of n_c subvectors $\lambda_{n,t,o}^v$, $\delta_{n,t,o}^v$, and $\dot{\delta}_{n,t,o}^v$, respectively; i.e.,

$$\lambda_{n,t,o} \equiv (\lambda_{n,t,o}^v)_{v=1}^{n_c} \in \mathfrak{R}^{n_s^2 n_c}, \quad \delta_{n,t,o} \equiv (\delta_{n,t,o}^v)_{v=1}^{n_c} \in \mathfrak{R}^{n_s^2 n_c},$$

and

$$\dot{\delta}_{n,t,o} \equiv (\dot{\delta}_{n,t,o}^v)_{v=1}^{n_c} \in \mathfrak{R}^{n_s^2 n_c}.$$

In a time stepping framework, the time superscript ℓ is added to each of the above variables. For instance, λ_n^ℓ is an $n_s^2 n_c$ -dimensional vector of normal contact forces at time instance t_ℓ , with $(\lambda_n^{\ell,v})_i$ for $i = 1, \dots, n_s^2$ being the (unknown) normal contact force on the system at the i th element in patch v .

³Note although this is reminiscent of the linear Kelvin-Voigt model, it is very different. The relationship between the total force (summation over elements of λ^v) to the gross deformation (penetration) is nonlinear.

Similarly, the system stiffness matrix K and the system damping matrix C , both of order $3n_s^2n_c \times 3n_s^2n_c$, are block diagonal concatenations of the respective contact patch stiffness matrices K^v and contact patch damping matrices C^v for $v = 1, \dots, n_c$. Note that the formulation for the lumped model described in [34] is obtained as a special case by setting $n_s = 1$. In this case, both the K and C are diagonal matrices.

The analytical expression for the influence function K^v for counterformal contacts can be derived from the elastic half-space theory and can be found in standard texts on elasticity and contact mechanics (see for example, [17, 25]). The relevant results are provided in Appendix A. The stiffness matrix K^v is the inverse of the compliance matrix Ξ^v whose entries are multiples of a small, positive scalar ε , the inverse of the Young's modulus of the material. Thus, we can write:

$$K \equiv \frac{1}{\varepsilon} \tilde{K},$$

for some symmetric positive definiteness matrix \tilde{K} that is independent of ε . With $C = 2\sqrt{K}$, we have

$$C = \frac{1}{\sqrt{\varepsilon}} \tilde{C},$$

where $\tilde{C} \equiv 2\sqrt{\tilde{K}}$. Concatenating the equation (6) over all the contact patches $v = 1, \dots, n_c$, and writing

$$\delta_{n,t,o}^\ell \equiv \delta_{n,t,o}(t_\ell), \quad \ell = 0, 1, \dots, N,$$

we obtain the following discrete-time algebraic equations:

$$\begin{aligned} \begin{pmatrix} \lambda_n^{\ell+1} \\ \lambda_t^{\ell+1} \\ \lambda_o^{\ell+1} \end{pmatrix} &= \begin{bmatrix} K_{nn} & K_{nt} & K_{no} \\ K_{tn} & K_{tt} & K_{to} \\ K_{on} & K_{ot} & K_{oo} \end{bmatrix} \begin{pmatrix} \delta_n^{\ell+1} \\ \delta_t^{\ell+1} \\ \delta_o^{\ell+1} \end{pmatrix} + \\ &\quad \frac{1}{h} \begin{bmatrix} C_{nn} & C_{nt} & C_{no} \\ C_{tn} & C_{tt} & C_{to} \\ C_{on} & C_{ot} & C_{oo} \end{bmatrix} \begin{pmatrix} \delta_n^{\ell+1} - \delta_n^\ell \\ \delta_t^{\ell+1} - \delta_t^\ell \\ \delta_o^{\ell+1} - \delta_o^\ell \end{pmatrix}. \end{aligned} \tag{7}$$

Note the stiffness matrix K and the damping matrix C are constants and therefore independent of $q^{\ell+1}$ and $\delta^{\ell+1}$. The system (7) is of order $3n_s^2n_c$, with each of the 18 block matrices (such as K_{nt} etc.) being an $n_s^2n_c$ block diagonal matrix with n_c diagonal blocks, one for each contact patch, and each such diagonal sub-block in turn being a square matrix of order n_s^2 .

To complete the description of the distributed compliance model, we note that each matrix $J\Psi_{n,t,o}(q)^T$ is of order $n_q \times n_s^2n_c$, with each column corresponding to an element (n_s^2 of these) in a contact patch (n_c of these). For convenience, we label these columns as $i = 1, \dots, n_s^2n_c$ and call each index a contact element.

2.3 Frictional contact conditions

To complete the formulation of the model, we need to include the contact conditions. In the normal direction, the contact condition at each $i = 1, \dots, n_s^2 n_c$ is governed by

$$0 \leq \lambda_{in}^{\ell+1} \perp s_{in}^{\ell+1} \geq 0.$$

where the \perp notation means perpendicularity and $s_{in}^{\ell+1}$ denotes the normal separation speed between two contacting bodies corresponding to the i th contact element,

$$s_{in}^{\ell+1} \equiv \frac{\delta_{in}^{\ell+1} - \delta_{in}^{\ell}}{h} + \frac{\nabla \Psi_{in}(q^{\ell})^T (q^{\ell+1} - q^{\ell})}{h}.$$

Unlike the contact constraints in the rigid-body model or the lumped compliant model, even in the same contact patch, each contact element has a different contact constraint Ψ_i depending on the local geometry over that contact patch. Figure 2 illustrates this for the normal springs associated with $J\Psi_n(q)^T$. When A and B are in contact, each spring has a line of action associated with it, and the i th line of action is described by the i th column of $J\Psi_n(q)^T$.

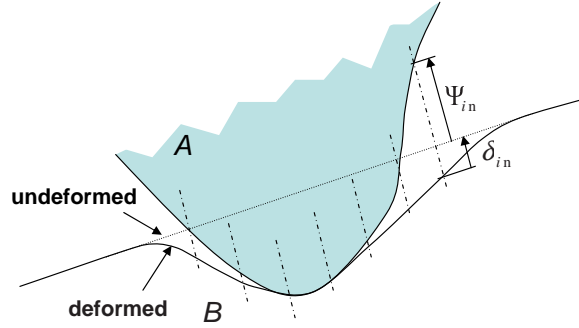


Figure 2: The separation between contact bodies depends on both the deformation δ_i and the contact constraint Ψ_i .

The tangential frictional conditions stipulate that, for each $i = 1, \dots, n_s^2 n_c$,

$$(\lambda_{it}^{\ell+1}, \lambda_{io}^{\ell+1}) \in \operatorname{argmin} \left\{ s_{it}^{\ell+1} \tilde{\lambda}_{it}^{\ell+1} + s_{io}^{\ell+1} \tilde{\lambda}_{io}^{\ell+1} : (\tilde{\lambda}_{it}^{\ell+1}, \tilde{\lambda}_{io}^{\ell+1}) \in \mathcal{F}_i(\mu_i \lambda_{in}^{\ell+1}) \right\},$$

where $\mu_i > 0$ is the friction coefficient at contact element i and $\mathcal{F}_i : \mathfrak{R}_+ \rightarrow \mathfrak{R}^2$ is the friction map at that contact, which is given by

$$\mathcal{F}_i(\tau) \equiv \begin{cases} \{(a, b) \in \mathfrak{R}^2 : \sqrt{a^2 + b^2} \leq \tau\} & \text{the Coulomb cone} \\ \{(a, b) \in \mathfrak{R}^2 : \max(|a|, |b|) \leq \tau\} & \text{a simple pyramid cone,} \end{cases}$$

for all $\tau \geq 0$. $s_{it,o}^{\ell+1}$ is the tangential slip velocity given by

$$s_{it}^{\ell+1} \equiv \frac{\delta_{it}^{\ell+1} - \delta_{it}^{\ell}}{h} + \frac{\nabla \Psi_{it}(q^{\ell})^T (q^{\ell+1} - q^{\ell})}{h}$$

and

$$s_{io}^{\ell+1} \equiv \frac{\delta_{io}^{\ell+1} - \delta_{io}^\ell}{h} + \frac{\nabla \Psi_{io}(q^\ell)^T (q^{\ell+1} - q^\ell)}{h}$$

Note that the slip velocities depend on both the deformations of the compliant elements and the rigid body motions.

3 Complementarity Formulations

In this section, we show that the discrete-time compliant contact model at time $t_{\ell+1}$ can be formulated as a mixed complementarity problem, provided that the friction maps \mathcal{F}_i correspond to either the Coulomb cone or its polyhedral approximations. The inputs to such a discrete-time complementarity problem are the quantities at time t_ℓ :

$$q^\ell, \quad \nu^\ell, \quad \lambda_{n,t,o}^\ell, \quad \text{and} \quad \delta_{n,t,o}^\ell,$$

and the unknown variables are the corresponding quantities at time $t_{\ell+1}$:

$$\left(q^{\ell+1}, \quad \nu^{\ell+1}, \quad \lambda_{n,t,o}^{\ell+1}, \quad \text{and} \quad \delta_{n,t,o}^{\ell+1} \right). \quad (8)$$

The key to the reformulation of the semi-implicit model is to use the dynamics equations of motion (3), the kinematics equation (4), and the force-displacement equations (7) to eliminate the state variables $q^{\ell+1}$, $\nu^{\ell+1}$, and $\delta_{n,t,o}^{\ell+1}$ in favor of $s^{\ell+1}$ and $\lambda^{\ell+1}$. In vector-matrix form, we have

$$\begin{pmatrix} \delta_n^{\ell+1} \\ \delta_t^{\ell+1} \\ \delta_o^{\ell+1} \end{pmatrix} = \begin{pmatrix} \delta_n^\ell \\ \delta_t^\ell \\ \delta_o^\ell \end{pmatrix} + h \begin{pmatrix} s_n^{\ell+1} \\ s_t^{\ell+1} \\ s_o^{\ell+1} \end{pmatrix} - \begin{bmatrix} J\Psi_n(q^\ell) \\ J\Psi_t(q^\ell) \\ J\Psi_o(q^\ell) \end{bmatrix} (q^{\ell+1} - q^\ell).$$

It is convenient for us to define the *system Jacobian matrix*:

$$\mathbf{W}(q^\ell) = \begin{bmatrix} W_n(q^\ell) \\ W_t(q^\ell) \\ W_o(q^\ell) \end{bmatrix} \equiv \begin{bmatrix} J\Psi_n(q^\ell) \\ J\Psi_t(q^\ell) \\ J\Psi_o(q^\ell) \end{bmatrix} G(q^\ell) \in \mathfrak{R}^{3n_s^2 n_c \times n_\nu}.$$

In terms of the matrix $\mathbf{W}(q^\ell)$, and substituting the kinematics equation (4) for $q^{\ell+1}$, we obtain

$$\begin{pmatrix} \delta_n^{\ell+1} \\ \delta_t^{\ell+1} \\ \delta_o^{\ell+1} \end{pmatrix} = \begin{pmatrix} \delta_n^\ell \\ \delta_t^\ell \\ \delta_o^\ell \end{pmatrix} + h \left\{ \begin{pmatrix} s_n^{\ell+1} \\ s_t^{\ell+1} \\ s_o^{\ell+1} \end{pmatrix} - \begin{bmatrix} W_n(q^\ell) \\ W_t(q^\ell) \\ W_o(q^\ell) \end{bmatrix} \nu^{\ell+1} \right\}. \quad (9)$$

Substituting this into the compliant force equation (7), we obtain

$$\begin{pmatrix} \lambda_n^{\ell+1} \\ \lambda_t^{\ell+1} \\ \lambda_o^{\ell+1} \end{pmatrix} \equiv \begin{bmatrix} K_{nn} & K_{nt} & K_{no} \\ K_{tn} & K_{tt} & K_{to} \\ K_{on} & K_{ot} & K_{oo} \end{bmatrix} \begin{pmatrix} \delta_n^\ell \\ \delta_t^\ell \\ \delta_o^\ell \end{pmatrix} + \begin{bmatrix} E_{nn} & E_{nt} & E_{no} \\ E_{tn} & E_{tt} & E_{to} \\ E_{on} & E_{ot} & E_{oo} \end{bmatrix} \left\{ \begin{pmatrix} s_n^{\ell+1} \\ s_t^{\ell+1} \\ s_o^{\ell+1} \end{pmatrix} - \begin{bmatrix} W_n(q^\ell) \\ W_t(q^\ell) \\ W_o(q^\ell) \end{bmatrix} \nu^{\ell+1} \right\}, \quad (10)$$

where

$$E \equiv \begin{bmatrix} E_{nn} & E_{nt} & E_{no} \\ E_{tn} & E_{tt} & E_{to} \\ E_{on} & E_{ot} & E_{oo} \end{bmatrix} \equiv h \begin{bmatrix} K_{nn} & K_{nt} & K_{no} \\ K_{tn} & K_{tt} & K_{to} \\ K_{on} & K_{ot} & K_{oo} \end{bmatrix} + \begin{bmatrix} C_{nn} & C_{nt} & C_{no} \\ C_{tn} & C_{tt} & C_{to} \\ C_{on} & C_{ot} & C_{oo} \end{bmatrix}.$$

Substituting (10) into the motion equation:

$$M(q^\ell) \nu^{\ell+1} = M(q^\ell) \nu^\ell + h f(t_\ell, q^\ell, \nu^\ell) + h \begin{bmatrix} W_n(q^\ell) \\ W_t(q^\ell) \\ W_o(q^\ell) \end{bmatrix}^T \begin{pmatrix} \lambda_n^{\ell+1} \\ \lambda_t^{\ell+1} \\ \lambda_o^{\ell+1} \end{pmatrix}, \quad (11)$$

we obtain

$$\mathbf{M}^\ell \nu^{\ell+1} = M(q^\ell) \nu^\ell + h f(t_\ell, q^\ell, \nu^\ell) + h \begin{bmatrix} W_n(q^\ell) \\ W_t(q^\ell) \\ W_o(q^\ell) \end{bmatrix}^T \left\{ \begin{bmatrix} K_{nn} & K_{nt} & K_{no} \\ K_{tn} & K_{tt} & K_{to} \\ K_{on} & K_{ot} & K_{oo} \end{bmatrix} \begin{pmatrix} \delta_n^\ell \\ \delta_t^\ell \\ \delta_o^\ell \end{pmatrix} + \begin{bmatrix} E_{nn} & E_{nt} & E_{no} \\ E_{tn} & E_{tt} & E_{to} \\ E_{on} & E_{ot} & E_{oo} \end{bmatrix} \begin{pmatrix} s_n^{\ell+1} \\ s_t^{\ell+1} \\ s_o^{\ell+1} \end{pmatrix} \right\},$$

where

$$\mathbf{M}^\ell \equiv M(q^\ell) + h \begin{bmatrix} W_n(q^\ell) \\ W_t(q^\ell) \\ W_o(q^\ell) \end{bmatrix}^T \begin{bmatrix} E_{nn} & E_{nt} & E_{no} \\ E_{tn} & E_{tt} & E_{to} \\ E_{on} & E_{ot} & E_{oo} \end{bmatrix} \begin{bmatrix} W_n(q^\ell) \\ W_t(q^\ell) \\ W_o(q^\ell) \end{bmatrix}.$$

is symmetric positive definite. Consequently,

$$\nu^{\ell+1} = \mathbf{r}^\ell + h (\mathbf{M}^\ell)^{-1} \begin{bmatrix} W_n(q^\ell) \\ W_t(q^\ell) \\ W_o(q^\ell) \end{bmatrix}^T \begin{bmatrix} E_{nn} & E_{nt} & E_{no} \\ E_{tn} & E_{tt} & E_{to} \\ E_{on} & E_{ot} & E_{oo} \end{bmatrix} \begin{pmatrix} s_n^{\ell+1} \\ s_t^{\ell+1} \\ s_o^{\ell+1} \end{pmatrix}, \quad (12)$$

where

$$\mathbf{r}^\ell \equiv (\mathbf{M}^\ell)^{-1} \left\{ M(q^\ell) \nu^\ell + h f(t_\ell, q^\ell, \nu^\ell) + h \begin{bmatrix} W_n(q^\ell) \\ W_t(q^\ell) \\ W_o(q^\ell) \end{bmatrix}^T \begin{bmatrix} K_{nn} & K_{nt} & K_{no} \\ K_{tn} & K_{tt} & K_{to} \\ K_{on} & K_{ot} & K_{oo} \end{bmatrix} \begin{pmatrix} \delta_n^\ell \\ \delta_t^\ell \\ \delta_o^\ell \end{pmatrix} \right\}.$$

Equation (12) expresses the system velocity $\nu^{\ell+1}$ in terms of the slip velocities. Substituting this equation into (10), we obtain

$$\begin{pmatrix} \lambda_n^{\ell+1} \\ \lambda_t^{\ell+1} \\ \lambda_o^{\ell+1} \end{pmatrix} = \begin{bmatrix} K_{nn} & K_{nt} & K_{no} \\ K_{tn} & K_{tt} & K_{to} \\ K_{on} & K_{ot} & K_{oo} \end{bmatrix} \begin{pmatrix} \delta_n^\ell \\ \delta_t^\ell \\ \delta_o^\ell \end{pmatrix} - \begin{bmatrix} \tilde{W}_n(q^\ell) \\ \tilde{W}_t(q^\ell) \\ \tilde{W}_o(q^\ell) \end{bmatrix} \mathbf{r}^\ell + \left\{ \begin{bmatrix} E_{nn} & E_{nt} & E_{no} \\ E_{tn} & E_{tt} & E_{to} \\ E_{on} & E_{ot} & E_{oo} \end{bmatrix} - \begin{bmatrix} \tilde{W}_n(q^\ell) \\ \tilde{W}_t(q^\ell) \\ \tilde{W}_o(q^\ell) \end{bmatrix} (h^{-1} \mathbf{M}^\ell)^{-1} \begin{bmatrix} \tilde{W}_n(q^\ell) \\ \tilde{W}_t(q^\ell) \\ \tilde{W}_o(q^\ell) \end{bmatrix}^T \right\} \begin{pmatrix} s_n^{\ell+1} \\ s_t^{\ell+1} \\ s_o^{\ell+1} \end{pmatrix}$$

where

$$\tilde{\mathbf{W}}(q^\ell) \equiv \begin{bmatrix} \tilde{W}_n(q^\ell) \\ \tilde{W}_t(q^\ell) \\ \tilde{W}_o(q^\ell) \end{bmatrix} \equiv \begin{bmatrix} E_{nn} & E_{nt} & E_{no} \\ E_{tn} & E_{tt} & E_{to} \\ E_{on} & E_{ot} & E_{oo} \end{bmatrix} \begin{bmatrix} W_n(q^\ell) \\ W_t(q^\ell) \\ W_o(q^\ell) \end{bmatrix}$$

The matrix

$$\mathbf{H}^\ell \equiv \begin{bmatrix} E_{nn} & E_{nt} & E_{no} \\ E_{tn} & E_{tt} & E_{to} \\ E_{on} & E_{ot} & E_{oo} \end{bmatrix} - \begin{bmatrix} \tilde{W}_n(q^\ell) \\ \tilde{W}_t(q^\ell) \\ \tilde{W}_o(q^\ell) \end{bmatrix} (h^{-1} \mathbf{M}^\ell)^{-1} \begin{bmatrix} \tilde{W}_n(q^\ell) \\ \tilde{W}_t(q^\ell) \\ \tilde{W}_o(q^\ell) \end{bmatrix}^T$$

plays an important role in the subsequent analysis. The proposition below establishes an important property of this matrix. Its proof is given in Appendix B.

Proposition 1 The matrix \mathbf{H}^ℓ is symmetric positive definite. □

Letting

$$\mathbf{p}^\ell \equiv \begin{bmatrix} K_{nn} & K_{nt} & K_{no} \\ K_{tn} & K_{tt} & K_{to} \\ K_{on} & K_{ot} & K_{oo} \end{bmatrix} \begin{pmatrix} \delta_n^\ell \\ \delta_t^\ell \\ \delta_o^\ell \end{pmatrix} - \begin{bmatrix} \tilde{W}_n(q^\ell) \\ \tilde{W}_t(q^\ell) \\ \tilde{W}_o(q^\ell) \end{bmatrix} \mathbf{r}^\ell,$$

we arrive at the following compact formulation of the compliant contact model:

$$\begin{pmatrix} \lambda_n^{\ell+1} \\ \lambda_t^{\ell+1} \\ \lambda_o^{\ell+1} \end{pmatrix} = \mathbf{p}^\ell + \mathbf{H}^\ell \begin{pmatrix} s_n^{\ell+1} \\ s_t^{\ell+1} \\ s_o^{\ell+1} \end{pmatrix} \quad (13)$$

$$0 \leq \lambda_n^{\ell+1} \perp s_n^{\ell+1} \geq 0$$

and for each $i = 1, \dots, n_s^2 n_c$,

$$(\lambda_{it}^{\ell+1}, \lambda_{io}^{\ell+1}) \in \operatorname{argmin} \left\{ s_{it}^{\ell+1} \tilde{\lambda}_{it}^{\ell+1} + s_{io}^{\ell+1} \tilde{\lambda}_{io}^{\ell+1} : (\tilde{\lambda}_{it}^{\ell+1}, \tilde{\lambda}_{io}^{\ell+1}) \in \mathcal{F}_i(\mu_i \lambda_{in}^{\ell+1}) \right\}.$$

From the solution of (13), the complete solution (8) of the problem at time $t_{\ell+1}$ can be determined by simple substitutions: $\nu^{\ell+1}$ from (11), $q^{\ell+1}$ from (4), and $\delta_{n,t,o}^{\ell+1}$ from (9).

3.1 The semi-implicit rigid-body model

For the purpose of subsequent comparison, it is useful for us to briefly review an associated multi-rigid-body model within the same time-stepping framework. Specifically, given the mass/inertia matrix $M(q)$, the system Jacobian matrix $\mathbf{W}(q)$, and the friction maps \mathcal{F}_i , the semi-implicit time-stepping multi-rigid-body frictional contact model are described by the following four sets of condition at all time steps t_ℓ for $\ell = 0, \dots, N-1$,

$$\begin{aligned} \nu^{\ell+1} &= \nu^\ell + hM(q^\ell)^{-1} [f(t_{\ell+1}, q^\ell, \nu^\ell) + W_n(q^\ell)^T \lambda_n + W_t(q^\ell)^T \lambda_t + W_o(q^\ell)^T \lambda_o] \\ q^{\ell+1} &= q^\ell + hG(q^\ell) \nu^{\ell+1} \end{aligned} \quad (14)$$

$$0 \leq \lambda_n^{\ell+1} \perp W_n(q^\ell) \nu^{\ell+1} \geq 0,$$

and for each $i = 1, \dots, n_c$,

$$(\lambda_{it}^{\ell+1}, \lambda_{io}^{\ell+1}) \in \operatorname{argmin} \left\{ s_{it}^{\ell+1} \lambda_{it}^{\ell+1} + s_{io}^{\ell+1} \lambda_{io}^{\ell+1} : (\lambda_{it}^{\ell+1}, \lambda_{io}^{\ell+1}) \in \mathcal{F}_i(\mu_i \lambda_{in}^{\ell+1}) \right\},$$

where $s_{it,o}^{\ell+1} \equiv W_{it,o}(q^\ell) \nu^{\ell+1}$. Much is known about the above discrete-time problem [2, 29, 37, 40]. In particular, under the assumption that, for all $\ell = 0, 1, \dots, N-1$,

$$\left. \begin{aligned} W_n(q^\ell)^T \lambda_n + W_t(q^\ell)^T \lambda_t + W_o(q^\ell)^T \lambda_o &= 0 \\ \lambda_n &\geq 0 \end{aligned} \right\} \Rightarrow \lambda_{n,t,o} = 0, \quad (15)$$

a discrete-time solution trajectory exists for the above rigid-body model. Moreover, it was argued in [29] that without this assumption or one of its variants (such as the more restrictive linear independence of all the vectors $\{W_{in}(q^\ell), W_{it}(q^\ell), W_{io}(q^\ell)\}_{i=1}^{n_c}$), the rigid-body model is unlikely to have solutions unless the external load $f(t, q, \nu)$ is properly restricted (see [30] for such exceptional cases). As we see in the next section, an advantage of a compliant contact model is that a solution exists for all external loads without the assumption (15).

4 Existence, Multiplicity, and Computation

Since \mathbf{H}^ℓ is positive definite, thus invertible, the first equation in the problem (13) can be written as:

$$\begin{pmatrix} s_n^{\ell+1} \\ s_t^{\ell+1} \\ s_o^{\ell+1} \end{pmatrix} = -(\mathbf{H}^\ell)^{-1} \mathbf{p}^\ell + (\mathbf{H}^\ell)^{-1} \begin{pmatrix} \lambda_n^{\ell+1} \\ \lambda_t^{\ell+1} \\ \lambda_o^{\ell+1} \end{pmatrix}.$$

The latter equation, along with the remaining conditions in (13) are of exactly the same mathematical form as the ‘‘all-rolling’’ multi-rigid-body model studied in [30]. Moreover, due to the positive definiteness of the matrix \mathbf{H}^ℓ , we can directly apply the results in the cited reference (see also Theorem 1 in [39]) and obtain the existence of a discrete-time solution trajectory to the compliant contact model, without any restriction on the original system Jacobian matrix $W(q)$. We summarize this existence result and show that such a trajectory must be unique when the friction coefficients are sufficiently small; see Appendix B for the proof. See Theorem 4 for a multiplicity result for arbitrary friction coefficients.

Theorem 2 For any fixed $h > 0$, the following two statements hold for the semi-implicit discrete-time, frictional compliant contact problem.

- (a) For every $\ell = 0, 1, \dots, N - 1$, the problem (13) has a solution; therefore, a discrete-time solution trajectory

$$\left\{ \left(q^{\ell+1}, \nu^{\ell+1}, \lambda_{n,t,o}^{\ell+1}, \delta_{n,t,o}^{\ell+1} \right)_{\ell=0}^{N-1} \right\}$$

exists for the compliant contact problem with friction.

- (b) There exists a scalar $\bar{\mu} > 0$ such that if $\mu_i \in [0, \bar{\mu}]$ for all $i = 1, \dots, n_s^2 n_c$, a unique solution trajectory exists. \square

4.1 Friction pyramid models

The numerical solution of (13) can be accomplished by complementarity methods. In what follows, we restrict the discussion to the case of the simple pyramid friction cone and show that the well-known Lemke’s complementary pivot algorithm [12] can successfully compute a solution of the discrete-time compliant contact model. For the extended treatment of other polygonal approximations of the friction cone, we can employ a technique similar to that in the Ph.D. thesis [23] for the multi-rigid-body problem. The details are omitted.

Write

$$-(\mathbf{H}^\ell)^{-1} \mathbf{p}^\ell \equiv \begin{pmatrix} b_n^\ell \\ b_t^\ell \\ b_o^\ell \end{pmatrix} \quad \text{and} \quad (\mathbf{H}^\ell)^{-1} \equiv \begin{bmatrix} J_{nn}^\ell & J_{nt}^\ell & J_{no}^\ell \\ J_{tn}^\ell & J_{tt}^\ell & J_{to}^\ell \\ J_{on}^\ell & J_{ot}^\ell & J_{oo}^\ell \end{bmatrix}.$$

With

$$\mathcal{F}_i(\mu_i \lambda_{in}^{\ell+1}) \equiv \left\{ (\lambda_{it}^{\ell+1}, \lambda_{io}^{\ell+1}) \in \mathfrak{R}^2 : \max(|\lambda_{it}^{\ell+1}|, |\lambda_{io}^{\ell+1}|) \leq \mu_i \lambda_{in}^{\ell+1} \right\},$$

introducing auxiliary variables $u_{t,o}^{\ell+1}$ and $v_{t,o}^{\ell+1}$, we can write the frictional condition:

$$(\lambda_{it}^{\ell+1}, \lambda_{io}^{\ell+1}) \in \operatorname{argmin} \left\{ s_{it}^{\ell+1} \lambda_{it}^{\ell+1} + s_{io}^{\ell+1} \lambda_{io}^{\ell+1} : (\lambda_{it}^{\ell+1}, \lambda_{io}^{\ell+1}) \in \mathcal{F}_i(\mu_i \lambda_{in}^{\ell+1}) \right\},$$

as the following equivalent complementarity conditions:

$$\begin{aligned} s_{it}^{\ell+1} &= u_{it}^{\ell+1} - v_{it}^{\ell+1} \\ s_{io}^{\ell+1} &= u_{io}^{\ell+1} - v_{io}^{\ell+1} \\ 0 \leq u_{it}^{\ell+1} &\perp \mu_i \lambda_{in}^{\ell+1} + \lambda_{it}^{\ell+1} \geq 0 \\ 0 \leq v_{it}^{\ell+1} &\perp \mu_i \lambda_{in}^{\ell+1} - \lambda_{it}^{\ell+1} \geq 0 \\ 0 \leq u_{io}^{\ell+1} &\perp \mu_i \lambda_{in}^{\ell+1} + \lambda_{io}^{\ell+1} \geq 0 \\ 0 \leq v_{io}^{\ell+1} &\perp \mu_i \lambda_{in}^{\ell+1} - \lambda_{io}^{\ell+1} \geq 0 \end{aligned} \tag{16}$$

Using the first two equations to eliminate the variables $s_{it}^{\ell+1}$ and $s_{io}^{\ell+1}$, we obtain the following mixed linear complementarity formulation (MLCP) in the variables

$$\lambda_{n,t,o}^{\ell+1}, \quad u_t^{\ell+1}, \quad v_t^{\ell+1}, \quad u_o^{\ell+1}, \quad v_o^{\ell+1}$$

for the compliant contact model at time $t_{\ell+1}$:

$$\begin{aligned} 0 &\leq \begin{pmatrix} \lambda_n^{\ell+1} \\ \lambda_t^{\ell+1} \\ \lambda_o^{\ell+1} \\ u_t^{\ell+1} \\ v_t^{\ell+1} \\ u_o^{\ell+1} \\ v_o^{\ell+1} \end{pmatrix} \perp \begin{pmatrix} b_n^\ell \\ b_t^\ell \\ b_o^\ell \\ 0 \\ 0 \\ 0 \\ 0 \end{pmatrix} + \mathbf{J}^\ell \begin{pmatrix} \lambda_n^{\ell+1} \\ \lambda_t^{\ell+1} \\ \lambda_o^{\ell+1} \\ u_t^{\ell+1} \\ v_t^{\ell+1} \\ u_o^{\ell+1} \\ v_o^{\ell+1} \end{pmatrix} \geq 0 \\ \text{free} & \quad \lambda_t^{\ell+1} = 0 \\ \text{free} & \quad \lambda_o^{\ell+1} = 0 \\ 0 &\leq u_t^{\ell+1} \geq 0 \\ 0 &\leq v_t^{\ell+1} \geq 0 \\ 0 &\leq u_o^{\ell+1} \geq 0 \\ 0 &\leq v_o^{\ell+1} \geq 0, \end{aligned} \tag{17}$$

where

$$\mathbf{J}^\ell \equiv \begin{bmatrix} J_{nn}^\ell & J_{nt}^\ell & J_{no}^\ell & 0 & 0 & 0 & 0 \\ J_{tn}^\ell & J_{tt}^\ell & J_{to}^\ell & -I & I & 0 & 0 \\ J_{on}^\ell & J_{ot}^\ell & J_{oo}^\ell & 0 & 0 & -I & I \\ \operatorname{diag}(\mu) & I & 0 & 0 & 0 & 0 & 0 \\ \operatorname{diag}(\mu) & -I & 0 & 0 & 0 & 0 & 0 \\ \operatorname{diag}(\mu) & 0 & I & 0 & 0 & 0 & 0 \\ \operatorname{diag}(\mu) & 0 & -I & 0 & 0 & 0 & 0 \end{bmatrix},$$

with $\text{diag}(\mu)$ being the $n_s^2 n_c \times n_s^2 n_c$ diagonal matrix of the friction coefficients at the contact elements. The matrix \mathbf{J}^ℓ is easily seen to be copositive on the cone $\mathfrak{R}_+^{n_s^2 n_c} \times \mathfrak{R}^{2n_s^2 n_c} \times \mathfrak{R}_+^{4n_s^2 n_c}$ that defines the MLCP (17). In order to obtain a pure LCP formulation of the compliant contact problem, we use the equation:

$$\begin{pmatrix} b_t^\ell \\ b_o^\ell \end{pmatrix} + \begin{bmatrix} J_{tn}^\ell \\ J_{on}^\ell \end{bmatrix} \lambda_n^{\ell+1} + \begin{bmatrix} J_{tt}^\ell & J_{to}^\ell \\ J_{ot}^\ell & J_{oo}^\ell \end{bmatrix} \begin{pmatrix} \lambda_t^{\ell+1} \\ \lambda_o^{\ell+1} \end{pmatrix} - \begin{pmatrix} u_t^{\ell+1} - v_t^{\ell+1} \\ u_o^{\ell+1} - v_o^{\ell+1} \end{pmatrix} = 0$$

to solve for the tangential forces $\lambda_{t,o}^{\ell+1}$, obtaining

$$\begin{pmatrix} \lambda_t^{\ell+1} \\ \lambda_o^{\ell+1} \end{pmatrix} = - \begin{bmatrix} J_{tt}^\ell & J_{to}^\ell \\ J_{ot}^\ell & J_{oo}^\ell \end{bmatrix}^{-1} \left\{ \begin{pmatrix} b_t^\ell \\ b_o^\ell \end{pmatrix} + \begin{bmatrix} J_{tn}^\ell \\ J_{on}^\ell \end{bmatrix} \lambda_n^{\ell+1} - \begin{pmatrix} u_t^{\ell+1} - v_t^{\ell+1} \\ u_o^{\ell+1} - v_o^{\ell+1} \end{pmatrix} \right\};$$

substituting this into (17), we get

$$\begin{aligned} 0 &\leq \begin{pmatrix} \lambda_n^{\ell+1} \\ u_t^{\ell+1} \\ v_t^{\ell+1} \\ u_o^{\ell+1} \\ v_o^{\ell+1} \end{pmatrix} \perp \begin{pmatrix} \tilde{b}_n^\ell \\ \tilde{b}_t^\ell \\ -\tilde{b}_t^\ell \\ \tilde{b}_o^\ell \\ -\tilde{b}_o^\ell \end{pmatrix} + \tilde{\mathbf{J}}^\ell \begin{pmatrix} \lambda_n^{\ell+1} \\ u_t^{\ell+1} \\ v_t^{\ell+1} \\ u_o^{\ell+1} \\ v_o^{\ell+1} \end{pmatrix} \geq 0 \\ & \hspace{15em} (18) \end{aligned}$$

where

$$\begin{aligned} \tilde{b}_n^\ell &\equiv b_n^\ell - J_{nt}^\ell \tilde{b}_t^\ell - J_{no}^\ell \tilde{b}_o^\ell, \quad \begin{pmatrix} \tilde{b}_t^\ell \\ \tilde{b}_o^\ell \end{pmatrix} \equiv - \begin{bmatrix} J_{tt}^\ell & J_{to}^\ell \\ J_{ot}^\ell & J_{oo}^\ell \end{bmatrix}^{-1} \begin{pmatrix} b_t^\ell \\ b_o^\ell \end{pmatrix}, \\ \tilde{\mathbf{J}}^\ell &\equiv \begin{bmatrix} \tilde{J}_{nn}^\ell & \tilde{J}_{nt}^\ell & -\tilde{J}_{nt}^\ell & \tilde{J}_{no}^\ell & -\tilde{J}_{no}^\ell \\ -\tilde{J}_{tn}^\ell & \tilde{J}_{tt}^\ell & -\tilde{J}_{tt}^\ell & \tilde{J}_{to}^\ell & -\tilde{J}_{to}^\ell \\ \tilde{J}_{tn}^\ell & -\tilde{J}_{tt}^\ell & \tilde{J}_{tt}^\ell & -\tilde{J}_{to}^\ell & \tilde{J}_{to}^\ell \\ -\tilde{J}_{on}^\ell & \tilde{J}_{ot}^\ell & -\tilde{J}_{ot}^\ell & \tilde{J}_{oo}^\ell & -\tilde{J}_{oo}^\ell \\ \tilde{J}_{on}^\ell & -\tilde{J}_{ot}^\ell & \tilde{J}_{ot}^\ell & -\tilde{J}_{oo}^\ell & \tilde{J}_{oo}^\ell \end{bmatrix} + \begin{bmatrix} 0 & 0 & 0 & 0 & 0 \\ \text{diag}(\mu) & 0 & 0 & 0 & 0 \\ \text{diag}(\mu) & 0 & 0 & 0 & 0 \\ \text{diag}(\mu) & 0 & 0 & 0 & 0 \\ \text{diag}(\mu) & 0 & 0 & 0 & 0 \end{bmatrix} \\ &\equiv \tilde{\mathbf{J}}_1^\ell + \tilde{\mathbf{J}}_2^\ell \end{aligned}$$

$$\tilde{J}_{nn}^\ell \equiv J_{nn}^\ell - \begin{bmatrix} J_{nt}^\ell & J_{no}^\ell \end{bmatrix} \begin{bmatrix} J_{tt}^\ell & J_{to}^\ell \\ J_{ot}^\ell & J_{oo}^\ell \end{bmatrix}^{-1} \begin{bmatrix} J_{tn}^\ell \\ J_{on}^\ell \end{bmatrix}$$

$$\begin{bmatrix} \tilde{J}_{\text{nt}}^\ell & \tilde{J}_{\text{no}}^\ell \end{bmatrix} \equiv \begin{bmatrix} J_{\text{nt}}^\ell & J_{\text{no}}^\ell \end{bmatrix} \begin{bmatrix} J_{\text{tt}}^\ell & J_{\text{to}}^\ell \\ J_{\text{ot}}^\ell & J_{\text{oo}}^\ell \end{bmatrix}^{-1}, \quad \begin{bmatrix} \tilde{J}_{\text{tt}}^\ell & \tilde{J}_{\text{to}}^\ell \\ \tilde{J}_{\text{ot}}^\ell & \tilde{J}_{\text{oo}}^\ell \end{bmatrix} \equiv \begin{bmatrix} J_{\text{tt}}^\ell & J_{\text{to}}^\ell \\ J_{\text{ot}}^\ell & J_{\text{oo}}^\ell \end{bmatrix}^{-1}.$$

We note that the matrices

$$\tilde{J}_{\text{nn}}^\ell \quad \text{and} \quad \begin{bmatrix} \tilde{J}_{\text{tt}}^\ell & \tilde{J}_{\text{to}}^\ell \\ \tilde{J}_{\text{ot}}^\ell & \tilde{J}_{\text{oo}}^\ell \end{bmatrix}$$

are positive definite.

We refer the reader to [12] for the description of Lemke's algorithm for solving LCPs. Exploiting the structure of the matrix \tilde{J}^ℓ , we can establish the following result, whose proof is given in Appendix B.

Theorem 3 Lemke's algorithm will compute a solution to the LCP (18). \square

Our next result asserts the finite multiplicity of solutions to the discrete-time, semi-implicit, frictional compliant contact problem for arbitrary positive friction coefficients $\mu_i, i = 1, \dots, n_s^2 n_c$. The same conclusion also applies to the multi-rigid-body model, which, to the best of our knowledge, is a new result even for this well studied problem. In order not to digress from the main topic of this paper, we will omit the details of the rigid model.

Theorem 4 There exists a finite set $\Omega \subset \mathfrak{R}_{++}^{n_s^2 n_c}$ of positive friction coefficients $\mu_i, i = 1, \dots, n_s^2 n_c$, such that the discrete-time, semi-implicit, frictional compliant contact problem has finitely many solution trajectories

$$\left\{ \left(q^{\ell+1}, \nu^{\ell+1}, \lambda_{\text{n,t,o}}^{\ell+1}, \delta_{\text{n,t,o}}^{\ell+1} \right)_{\ell=0}^{N-1} \right\}$$

for each fixed but arbitrary $\mu \notin \Omega$. \square

Remark. It is possible to show that for every $\mu \in \Omega$, the solution trajectories to the semi-implicit compliant contact model must be bounded (while again no such boundedness is claimed for the auxiliary u and v variables). We omit the details of the proof.

5 Limit Analysis of a Lumped Model

The analysis so far deals with the discrete-time, semi-implicit, frictional compliant contact problem corresponding to a given (but arbitrary) stiffness matrix K . In this section, we carry out a limit analysis of the solutions to the model by letting the Young's modulus of the system tend to infinity, i.e., by letting the scalar ε , which is the reciprocal of the Young modulus, tend to zero. Throughout the analysis, the time step h is held fixed; hence, the analysis is being made in a discrete-time framework. A similar analysis has been suggested for frictionless impacts [1], where a limit analysis of results produced by a fixed-step time stepping algorithm

for regularized contact models (which can be used for rigid-body dynamic simulation) shows that the trajectory converges to that produced by rigid-body impact models for frictionless impacts.

Our limit analysis is restricted to a lumped compliant contact model where $n_s = 1$. Although it is possible to extend the analysis to the distributed model when $\nabla\Psi_{i\text{nto}}$ are the same for all i belonging to the same contact patch, we prefer to simplify the analysis by focusing on the lumped model. (In the said extension, the result would pertain to the sum of the contact forces at each contact patch.) For the analysis to follow, we need several conditions, the first two of which, (A1) and (A2), are as follows.

(A1) The stiffness matrix K and the damping matrix C , both dependent on ε , are such that

$$\lim_{\varepsilon \downarrow 0} \varepsilon E$$

exists and is positive definite, where $E \equiv hK + C$.

(A2) The initial conditions, allowed to depend on ε , satisfy

$$\limsup_{\varepsilon \downarrow 0} \|(q^0, \nu^0)\| < \infty \quad \text{and} \quad \limsup_{\varepsilon \downarrow 0} \frac{1}{\sqrt{\varepsilon}} \|\delta_{n,t,o}^0\| < \infty.$$

Assumption (A1) implies

$$\limsup_{\varepsilon \downarrow 0} \varepsilon \|K\| < \infty \quad \text{and} \quad \limsup_{\varepsilon \downarrow 0} \varepsilon \|C\| < \infty.$$

The second limit in (A2) holds if, for example, the initial deformations are zero.

The following lemma, whose proof is given in Appendix B, establishes the boundedness of the velocities $\{\nu^\ell\}$ and the configurations $\{q^\ell\}$ at all time steps as ε tends to zero (part (c)). Part (a) of this lemma is useful for relating the compliant model to the rigid model (see Theorem 6); part (b) and (A2) together imply that for all $\ell = 0, 1, \dots, N$,

$$\lim_{\varepsilon \downarrow 0} \delta_{n,t,o}^\ell = 0. \tag{19}$$

Part (d) asserts that the resultant forces at the center of mass due to the contacts must be bounded.

Lemma 5 Let $(\nu^{\ell+1,\varepsilon}, q^{\ell+1,\varepsilon}, \lambda_{n,t,o}^{\ell+1,\varepsilon}, \delta_{n,t,o}^{\ell+1,\varepsilon}, s_{n,t,o}^{\ell+1,\varepsilon})$, for $\ell = 0, 1, \dots, N-1$, denote any discrete-time solution of the semi-implicit compliant contact model. Under assumptions (A1) and (A2), it holds that

$$(a) \quad \limsup_{\varepsilon \downarrow 0} \frac{1}{\sqrt{\varepsilon}} \left\| s_{n,t,o}^{\ell+1,\varepsilon} - W_{n,t,o}(q^{\ell,\varepsilon}) \nu^{\ell+1,\varepsilon} \right\| < \infty;$$

$$(b) \quad \limsup_{\varepsilon \downarrow 0} \frac{1}{\sqrt{\varepsilon}} \|\delta_{n,t,o}^{\ell+1,\varepsilon}\| < \infty;$$

$$(c) \limsup_{\varepsilon \downarrow 0} \|(q^{\ell+1,\varepsilon}, \nu^{\ell+1,\varepsilon})\| < \infty;$$

$$(d) \limsup_{\varepsilon \downarrow 0} \|W_n(q^{\ell,\varepsilon})^T \lambda_n^{\ell+1,\varepsilon} + W_t(q^{\ell,\varepsilon})^T \lambda_t^{\ell+1,\varepsilon} + W_o(q^{\ell,\varepsilon})^T \lambda_o^{\ell+1,\varepsilon}\| < \infty,$$

for all $\ell = 0, 1, \dots, N-1$. □

The above lemma does not address the boundedness of the trajectory of compliant contact forces $\{(\lambda_{n,t,o}^{\ell,\varepsilon})_{\ell=1}^N\}$ as $\varepsilon \downarrow 0$, nor does the lemma assert what the accumulation points, which must exist, of the (discrete-time) state trajectory $\{(q^{\ell,\varepsilon}, \nu^{\ell,\varepsilon})_{\ell=0}^N\}$ are as $\varepsilon \downarrow 0$. Theorem 6 below deals with these two issues; in particular, it identifies any accumulation point of the state trajectory as a solution of a corresponding discrete-time rigid-body model. Before presenting the theorem, we explain the key condition that we impose in order to ensure the boundedness of the compliant contact forces. To begin, let $\{\varepsilon_k\}$ be any sequence of positive scalars converging to zero. The sequence of state variables $\{(q^{\ell,\varepsilon_k}, \nu^{\ell,\varepsilon_k})_{\ell=0}^N\}$ is bounded; it therefore has an accumulation point; let $(q^{\ell,\infty}, \nu^{\ell,\infty})_{\ell=0}^N$ be any such point and let κ be an infinite subset of positive integers such that

$$\lim_{k(\in \kappa) \rightarrow \infty} (q^{\ell,\varepsilon_k}, \nu^{\ell,\varepsilon_k}) = (q^{\ell,\infty}, \nu^{\ell,\infty}), \quad \forall \ell = 0, 1, \dots, N.$$

Since $s_n^{\ell+1,\varepsilon_k} \geq 0$ for all k , by taking limits $k \rightarrow \infty$ and using part (a) of Lemma 5, we deduce

$$W_n(q^{\ell,\infty}) \nu^{\ell+1,\infty} \geq 0, \quad \forall \ell = 0, 1, \dots, N-1.$$

Clearly if $W_{in}(q^{\ell,\infty}) \nu^{\ell+1,\infty} > 0$ at some contact point i , then

$$s_{in}^{\ell+1,\varepsilon_k} = 0 = \lambda_{in}^{\ell+1,\varepsilon_k} = \lambda_{it}^{\ell+1,\varepsilon_k} = \lambda_{io}^{\ell+1,\varepsilon_k}$$

for all $k \in \kappa$ sufficiently large. It is natural to call such a contact point i *breaking* relative to the pair $(q^{\ell+1,\infty}, \nu^{\ell+1,\infty})$. Clearly the contact forces $(\lambda_{in}^{\ell+1,\varepsilon_k}, \lambda_{it}^{\ell+1,\varepsilon_k}, \lambda_{io}^{\ell+1,\varepsilon_k})$ at a breaking contact point must converge to zero. Hence we need to concentrate only on the convergence of these forces at a non-breaking contact point. For this reason, we let

$$\mathcal{I}_\ell \equiv \{i : W_{in}(q^{\ell,\infty}) \nu^{\ell+1,\infty} = 0\}$$

be the set of “active contacts” corresponding to the pair $(q^{\ell+1,\infty}, \nu^{\ell+1,\infty})$ at time $t_{\ell+1}$. We further let

$$\mathcal{J}_\ell \equiv \{i \in \mathcal{I}_\ell : W_{it}(q^{\ell,\infty}) \nu^{\ell+1,\infty} = W_{io}(q^{\ell,\infty}) \nu^{\ell+1,\infty} = 0\}$$

be the set of *rolling contacts* at the same pair. The sufficient condition to ensure the boundedness of the corresponding sequence of contact forces $\{(\lambda_{n,t,o}^{\ell+1,\varepsilon_k})_{\ell=0}^{N-1} : k \in \kappa\}$ is that for each $\ell = 0, 1, N-1$, the system gradients in the normal direction n:

$$\left\{ W_{in}(q^{\ell,\infty}) \right\}_{i \in \mathcal{I}_\ell}$$

are “positively linearly independent” of the system gradients in the two tangential directions t and o :

$$\left\{ W_{jt}(q^{\ell,\infty}), W_{jo}(q^{\ell,\infty}) \right\}_{j \in \mathcal{J}_\ell},$$

which themselves are linearly independent. Specifically, this sufficient condition stipulates that the following algebraic implication holds for all $\ell = 0, 1, \dots, N - 1$:

$$\left. \begin{aligned} \sum_{i \in \mathcal{I}_\ell} W_{in}(q^{\ell,\infty})^T \lambda_{in} + \sum_{j \in \mathcal{J}_\ell} \left[W_{jt}(q^{\ell,\infty})^T \lambda_{jt} + W_{jo}(q^{\ell,\infty})^T \lambda_{jo} \right] &= 0 \\ \lambda_{in} &\geq 0, \quad i \in \mathcal{I}_\ell \\ (\lambda_{jt}, \lambda_{jo}) &\in \mathcal{F}_j(\mu_j \lambda_{jn}), \quad j \in \mathcal{J}_\ell \end{aligned} \right\} \quad (20)$$

$$\Rightarrow \begin{cases} \lambda_{in} = 0, & i \in \mathcal{I}_\ell \\ \lambda_{jt} = 0 = \lambda_{jo}, & j \in \mathcal{J}_\ell. \end{cases}$$

Incidentally, the above implication is considerably weaker than (15) because the former pertains only to the active contact gradients whereas the latter involves all contact gradients.

Once we have established that the force sequence is bounded, we can then show that the pairs of state variables $(q^{\ell,\infty}, \nu^{\ell,\infty})_{\ell=0}^N$ must be a solution to the corresponding rigid-body model with the same input data. We summarize the above discussion in the following main result whose proof is given in Appendix B.

Theorem 6 Let $\{\varepsilon_k\}$ be a sequence of positive scalars converging to zero. Suppose that, for all $\ell = 0, 1, \dots, N$,

$$\lim_{k \rightarrow \infty} (q^{\ell,\varepsilon_k}, \nu^{\ell,\varepsilon_k}) = (q^{\ell,\infty}, \nu^{\ell,\infty}).$$

If the implication (20) holds for all $\ell = 0, 1, \dots, N - 1$, then the force trajectory $\left\{ (\lambda_{n,t,o}^{\ell+1,\varepsilon_k})_{\ell=0}^{N-1} \right\}$ is bounded; moreover, if κ is any infinite subset of positive integers such that, for all $\ell = 0, 1, \dots, N - 1$,

$$\lim_{k(\in \kappa) \rightarrow \infty} \lambda_{n,t,o}^{\ell+1,\varepsilon_k} = \lambda_{n,t,o}^{\ell+1,\infty},$$

then for all $\ell = 0, 1, \dots, N - 1$, the limiting tuple $(q^{\ell+1,\infty}, \nu^{\ell+1,\infty}, \lambda_{n,t,o}^{\ell+1,\infty})$ satisfies the following conditions:

$$M(q^{\ell,\infty})\nu^{\ell+1,\infty} = M(q^{\ell,\infty})\nu^{\ell,\infty} + h f(t_{\ell+1}, q^{\ell,\infty}, \nu^{\ell,\infty}) + h \begin{bmatrix} W_n(q^{\ell,\infty}) \\ W_t(q^{\ell,\infty}) \\ W_o(q^{\ell,\infty}) \end{bmatrix}^T \begin{pmatrix} \lambda_n^{\ell+1,\infty} \\ \lambda_t^{\ell+1,\infty} \\ \lambda_o^{\ell+1,\infty} \end{pmatrix}$$

$$q^{\ell+1,\infty} = q^{\ell,\infty} + h G(q^{\ell,\infty})\nu^{\ell+1,\infty}$$

$$0 \leq \lambda_n^{\ell+1,\infty} \perp W_n(q^{\ell,\infty})\nu^{\ell+1,\infty} \geq 0,$$

and for each $i = 1, \dots, n_c$,

$$(\lambda_{it}^{\ell+1,\infty}, \lambda_{io}^{\ell+1,\infty}) \in \operatorname{argmin} \left\{ s_{it}^{\ell+1,\infty} \lambda_{it}^{\ell+1} + s_{io}^{\ell+1,\infty} \lambda_{io}^{\ell+1} : (\lambda_{it}^{\ell+1}, \lambda_{io}^{\ell+1}) \in \mathcal{F}_i(\mu_i \lambda_{in}^{\ell+1,\infty}) \right\},$$

where $s_{it,o}^{\ell+1,\infty} \equiv W_{it,o}(q^{\ell,\infty}) \nu^{\ell+1,\infty}$. □

6 Numerical Implementation and Results

In this section, we first present an algorithm that implements the discrete-time, distributed compliant contact model for dynamic simulation described in Section 2. We then illustrate the application of this algorithm by solving a planar frictional contact problem.

The following simulation algorithm computes the states variables $(q^{\ell+1}, \nu^{\ell+1}, \lambda^{\ell+1}, \delta^{\ell+1})$ of the multibody system given the known states $(q^\ell, \nu^\ell, \lambda^\ell, \delta^\ell)$ obtained from the previous time step. There are four computational steps:

1. Determine the contact location from the system configuration (q^ℓ, \dot{q}^ℓ) and the geometry of the contacting objects. Discretize the surface patch surrounding the contact point into $n_s \times n_s$ elements.
2. Solve the MLCP (17) for contact forces $\lambda_{n,t,o}^{\ell+1}$ and the separation speeds $s_{n,t,o}^{\ell+1}$. In practice, we can solve the LCP (18) instead. Our numerical implementation uses Lemke's algorithm for solving the LCP (18).
3. Solve for the states variables $\nu^{\ell+1}$, $q^{\ell+1}$, and $\delta^{\ell+1}$, using equations (3), (4), and (9), respectively
4. Repeat steps 1–3 for the next time step.

Our test problem is a 2-dimensional elliptical object contacting a horizontal surface as shown in Figure 3. Rolling or sliding may occur between the object and the surface depending on the coefficient of friction. The generalized coordinates of the ellipse, $q \equiv (x, y, \theta)$, consist of (x, y) , the coordinates of the center of mass, and θ , the angle of the major axis of the ellipse from the horizontal surface. The object used in the test has a major axis of 0.2m and a minor axis of 0.1m. The mass of the object is 0.05kg. The moment of inertia about the center of mass is $1.5 \times 10^{-4} \text{kg}\cdot\text{m}^2$. The coefficient of friction is $\mu = 0.2$. The number of spring-damper sets is $n_s = 3$ and the distance between the reference point of the adjacent spring-damper units is $\rho_0 = 10^{-6} \text{m}$. Other than the contact forces, gravity is the only external force acting on the object. The initial configuration of the ellipse is $q^0 = (0, 0.0975, 75^\circ)$ with the object touching the surface. In this test problem, the Jacobian matrices of the distributed model ($n_s = 3$) can be expressed as

$$J\Psi_n^T(q) = \begin{pmatrix} 0 & 0 & 0 \\ 1 & 1 & 1 \\ p_{1,x}(q) & p_{2,x}(q) & p_{3,x}(q) \end{pmatrix}, \quad J\Psi_t^T(q) = \begin{pmatrix} 1 & 1 & 1 \\ 0 & 0 & 0 \\ p_{1,y}(q) & p_{2,y}(q) & p_{3,y}(q) \end{pmatrix},$$

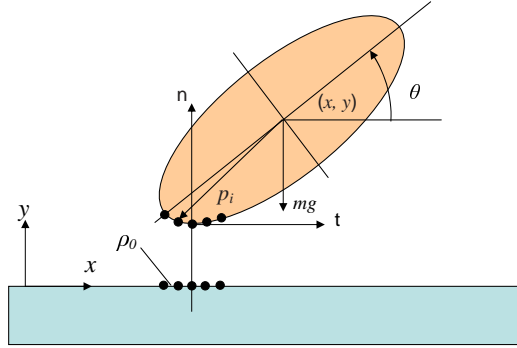


Figure 3: Contact between an elliptical object and a horizontal surface

where $p_{i,x}$ and $p_{i,y}$ denote, respectively, the x and y components of the position vector of the i th contact element.

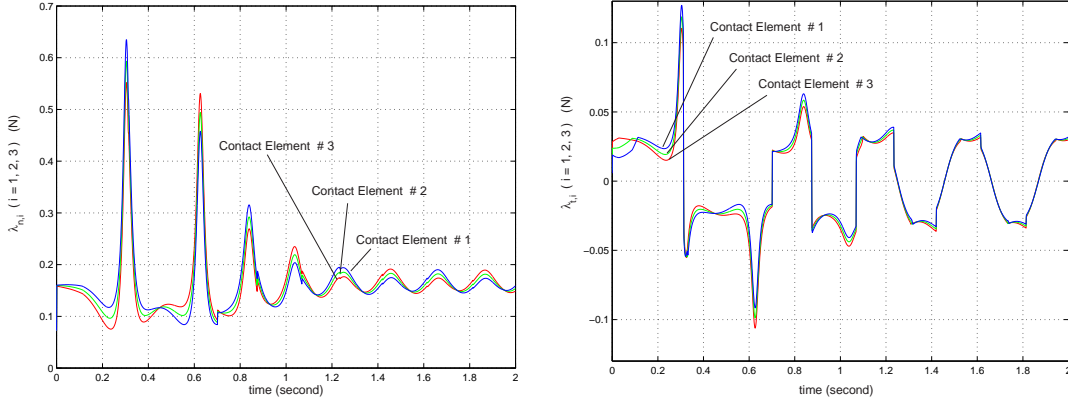
We apply our simulation algorithm to this test problem and the results are reported in Figure 4. In this test, we set the compliance parameter $\epsilon = 10^{-10}(\text{m}^2/\text{N})$. The number of spring sets is $n_s = 3$ and they are labelled as contact elements 1, 2, and 3 from left to right (refer to Figure 3). The time step h is 10^{-4} seconds and the number of time steps is $N = 2 \times 10^4$. The object starts with the rolling state, after several transitions between rolling and sliding, the object settles in a condition of rolling. This steady rolling state causes a ripple in the normal contact force and the offset is roughly equal to the weight of the object. The distribution of the contact forces and friction forces at different contact elements are depicted in Figure 4(a) and (b) respectively. Figure 4(c) shows the transitions between the rolling and sliding contact states. A zoomed-in view at one of these transitions reveals the so-called microslip phenomenon, that is, during this particular transition, the sliding starts at the rightmost contact element first and gradually shifts to the left elements on the contact patch.

To demonstrate the convergence of the solution of the distributed compliant contact model to the rigid-body solution, we simulate the motion of the object using the former model with different ϵ ($\epsilon = 10^{-11}, 10^{-10}, 10^{-9}$) and compare the results with the solutions of the semi-implicit rigid-body model described in equation (14). The time step h is set to be 10^{-4} seconds for both models. The snapshots of the object motion is depicted in Figure 5(a). In this example, the rigid-body model always yields unique solutions for the accelerations and the contact forces.

The history of the normal displacement at the center of the mass is shown in Figure 5(b). Figure 5(c,d) show the comparisons between the sum of the contact forces by using the distributed compliant model and the results from rigid-body LCP model in the normal and tangential directions, respectively. We can see that as the stiffness of the object increases, both the motion trajectories and the force histories of the compliant model converge to the respective rigid-body solutions.

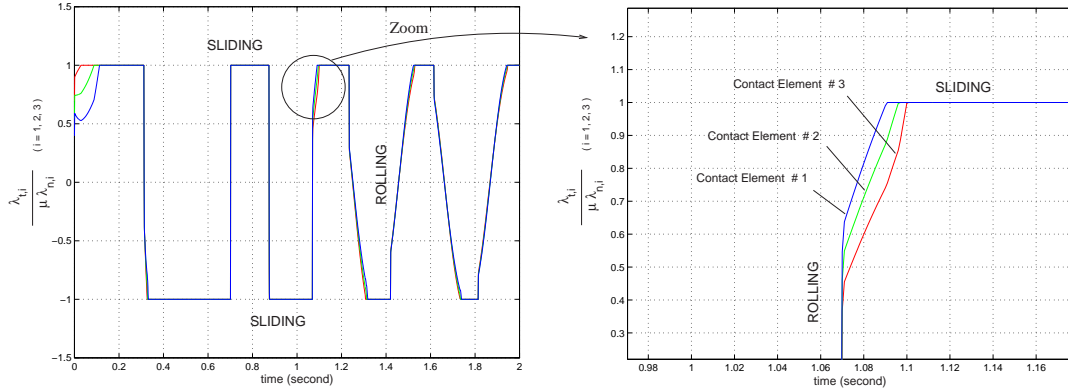
7 Conclusion

Extending the Ph.D. thesis of the first author [33], this paper presents for the first time a formal, discrete time-stepping model for dynamic simulation with compliant, frictional contacts.



(a) Distribution of the normal contact forces over the contact patch.

(b) Distribution of the friction forces over the contact patch.



(c) The (normalized) tangential forces at each contact element demonstrating the microslip phenomenon.

Figure 4: Simulation results using the the distributed compliant model.

Our contact model incorporates distributed parameter models of the contact interactions using viscoelastic constitutive laws and pointwise Coulomb-like friction laws. The main contribution of this paper is a set of results that (a) show the existence and uniqueness of solutions for this model (Theorem 3), and for the case of a friction pyramid cone, the finite multiplicity of solutions (Theorem 4); and (b) the convergence of the solution trajectory to that obtained by the rigid body dynamic model as the compliance tends to zero (Theorem 6). A related contribution is the demonstration that Lemke’s algorithm can solve the linear complementarity problem formulation of the time-stepping compliant model (Section 6).

From a practical standpoint it is clear that the distributed compliant contact model is more complex than the rigid-body model. The former requires more parameters to describe the local behaviors of the contacts, and more importantly from an algorithmic standpoint, it increases the computational cost by a factor of n_s^2 . However, the distributed compliant model can model

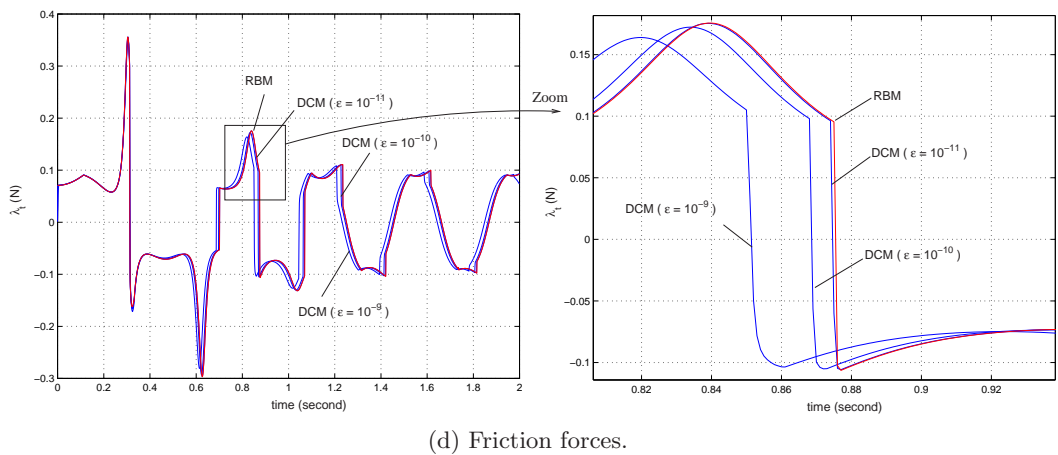
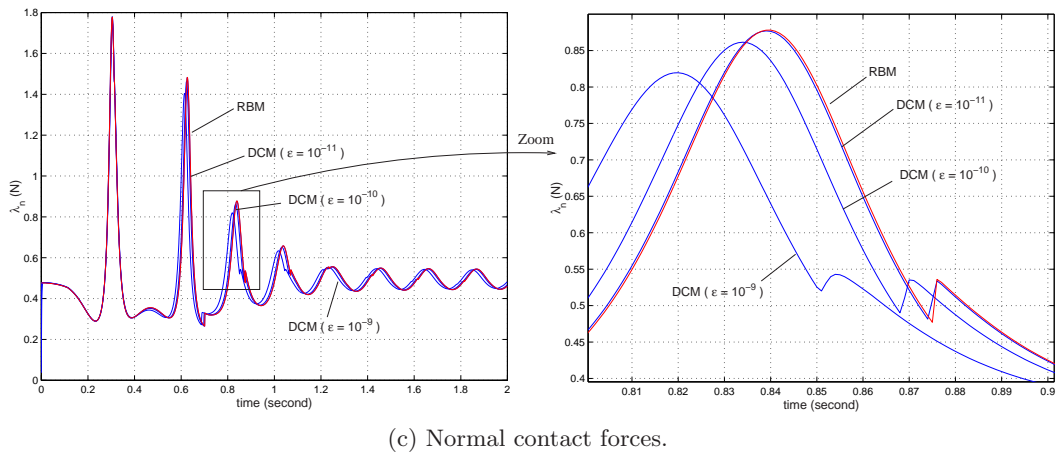
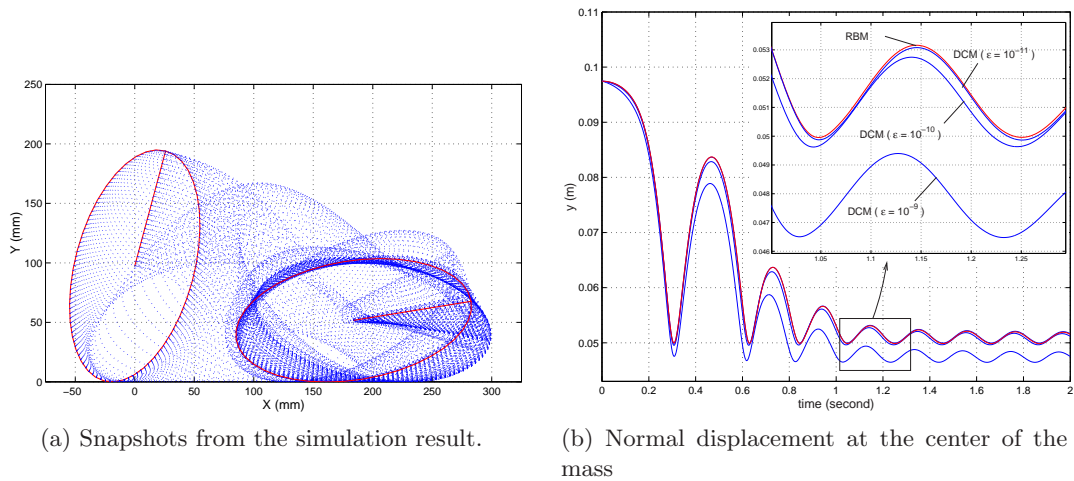


Figure 5: Convergence of the distributed compliant model (DCM) to the rigid-body model (RBM)

the stress distribution and microslip thus allowing more complex frictional models. Moreover, the compliant model does allow solutions for problems that are statically indeterminate where rigid-body models do not provide solutions in such situations. The methodology presented in this paper has potential applications in the dynamic simulation of systems consisting of rigid and deformable bodies. Examples of such systems can be found in medical robotics [22] and virtual environments [10].

Acknowledgements

The authors would like to thank Professor David Stewart, University of Iowa, for discussions on time-stepping methods and Professor Michael Ferris, University of Wisconsin, Madison, for providing and supporting PATH [13].

References

- [1] M. Anitescu. A fixed time step approach for multi-body dynamics with contact and friction. Division of Mathematics and Computer Science, Argonne National Laboratory, 2003. Under review.
- [2] M. Anitescu and F. Potra. Formulating dynamic multi-rigid-body contact problems with friction as solvable linear complementarity problems. *Nonlinear Dynamics*, 14, pp. 231–247, 1997.
- [3] M. Anitescu, F. Potra, and D. Stewart. Time-stepping for three-dimensional rigid body dynamics. *Methods in Applied Mechanics and Engineering*, 17(3–4), pp. 183–197, 1999.
- [4] M. Anitescu and F. A. Potra. A time-stepping method for stiff multibody dynamics with contact and friction. *International Journal of Numerical Methods in Engineering*, 55(7), pp. 753–784, 2002.
- [5] B. Armstrong-Hélouvy. *Control of Machines with Friction*. Kluwer Academic Publishers, Boston, MA, 1991.
- [6] D. Baraff. Fast contact force computation for nonpenetrating rigid bodies. *Computer Graphics*, 28, pp. 23–34, 1994.
- [7] K. J. Bathe. *Finite Element Procedures*. Prentice-Hall, Englewood Cliffs, NJ, 1995.
- [8] R. M. Brach. Rigid body collisions. *Journal of Applied Mechanics*, 56, pp. 133–138, 1989.
- [9] B. Brogliato. *Nonsmooth Impact Mechanics - Models, Dynamics, and Control*. Springer-Verlag, London, 1996. Lecture Notes in Control and Information Sciences.
- [10] M.C. Cavusoglu and F. Tendick. Multirate Simulation for High Fidelity Haptic Interaction with Deformable Objects in Virtual Environments. In *Proceedings of the 2000 IEEE International Conference on Robotics and Automation*, pp. 2458–2465, 2000.
- [11] A. Chatterjee and A. Ruina. Two interpretations of rigidity in rigid body collisions. *Journal of Applied Mechanics*, 65(4), pp. 939–951, 1997.
- [12] R. W. Cottle, J. S. Pang, and R. E. Stone. *The Linear Complementarity Problem*. Academic Press, Inc., San Diego, CA, 1992.
- [13] S. P. Dirkse and M. C. Ferris. The path solver: A non-monotone stabilization scheme for mixed complementarity problems. *Optimization Methods and Software*, 5, pp. 123–156, 1995.

- [14] R. Fearing and T. Binford. Using a cylindrical tactile sensor for determining curvature. In *Proceedings of the 1988 IEEE International Conference on Robotics and Automation*, pp. 254–260, 1988.
- [15] S. Goyal, E. N. Pinson, and F. W. Sinden. Simulation of dynamics of interacting rigid bodies including friction i: General problem and contact model. *Engineering with Computers*, 10, pp. 162–174, 1994.
- [16] W. S. Howard and V. Kumar. A minimum principle for the dynamic analysis of systems with frictional contacts. In *Proceedings of the 1993 IEEE International Conference on Robotics and Automation*, pp. 437–442, 1993.
- [17] K. L. Johnson. *Contact Mechanics*. Cambridge University Press, Cambridge, UK, 1985.
- [18] J. Kalker. *Three-Dimensional Elastic Bodies in Rolling Contact*. Kluwer Academic Publishers, Dordrecht, The Netherlands, 1990.
- [19] N. Kikuchi and J. T. Oden. *Contact Problems in Elasticity: A Study of Variational Inequalities and Finite Element Methods*. Society for Industrial and Applied Mathematics, Philadelphia, PA, 1988.
- [20] E. Kokkevis and D. Metaxas. Efficient dynamic constraints for animating articulated figures. *Multi-body System Dynamics*, 2, pp. 89–114, 1998.
- [21] P. R. Kraus, A. Fredriksson, and V. Kumar. Modeling of frictional contacts for dynamic simulation. In *Proceedings of IROS 1997 Workshop on Dynamic Simulation: Methods and Applications*, 1997.
- [22] C. Laugier, D. d’Aulignac, and F. Boux de Casson. Modeling human tissues for medical simulators. In *Proceedings of the IEEE-RSJ International Conference on Intelligent Robots and Systems*, 2000.
- [23] G. Lo. *Complementarity Problems in Robotics*. PhD thesis, Department of Mathematical Sciences, The Johns Hopkins University, Baltimore, MD, 1996.
- [24] P. Lötstedt. Coulomb friction in two-dimensional rigid body systems. *Zeitschrift für Angewandte Mathematik und Mechanik*, Bd.61, pp. 605–615, 1981.
- [25] A. I. Lur’e. *Three-Dimensional Problems of the Theory of Elasticity*. Interscience Publishers, New York, NY, 1964.
- [26] D. B. Marghitu and Y. Hurmuzlu. Three-dimensional rigid body collisions with multiple contact points. *Journal of Applied Mechanics*, 62, pp. 725–732, 1995.
- [27] B. Mirtich, Y. Zhuang, K. Goldberg, J. Craig, R. Zanutta, B. Carlisle, and J. Canny. Estimating pose statistics for robotic part feeders. In *Proceedings of the 1996 IEEE International Conference on Robotics and Automation*, pp. 1140–1146, 1996.
- [28] J. T. Oden and E. B. Pires. Nonlocal and nonlinear friction laws and variational principles for contact problems in elasticity. *Journal of Applied Mechanics*, 50(1), pp. 67–76, 1983.
- [29] J. S. Pang and D. Stewart. A unified approach to discrete frictional contact problems. *International Journal of Engineering Science*, 37, pp. 1747–1768, 1999.
- [30] J. S. Pang and J. C. Trinkle. Complementarity formulations and existence of solutions of dynamic multi-rigid-body contact problems with coulomb friction. *Mathematical Programming*, 73, pp. 199–226, 1996.
- [31] B. Paul and J. Hashemi. Contact pressure on closely conforming elastic bodies. *Journal of Applied Mechanics*, pp. 543–548, 1981.

- [32] P. R. Sinha and J. M. Abel. A contact stress model for multifingered grasps of rough objects. In *Proceedings of the 1990 IEEE International Conference on Robotics and Automation*, pp. 1040–1045, 1990.
- [33] P. Song. *Modeling, Analysis and Simulation of Multibody Systems with Contact and Friction*. PhD thesis, Department of Mechanical Engineering and Applied Mechanics, University of Pennsylvania, Philadelphia, PA, 2002.
- [34] P. Song, P. Kraus, V. Kumar, and P. Dupont. Analysis of rigid-body dynamic models for simulation of systems with frictional contacts. *Journal of Applied Mechanics*, 68, pp. 118–128, 2001.
- [35] D. Stewart. Convergence of a time-stepping scheme for rigid-body dynamics and resolution of painlevé’s problem. *Archive for Rational Mechanics and Analysis*, 145, pp. 215–260, 1998.
- [36] D. Stewart. Rigid-body dynamics with friction and impact. *SIAM Review*, 42, pp. 3–39, 2000.
- [37] D. Stewart and J. Trinkle. An implicit time-stepping scheme for rigid-body dynamics with inelastic collisions and coulomb friction. *International Journal of Numerical Methods in Engineering*, 39, pp. 2673–2691, 1996.
- [38] J. Trinkle, J.-S. Pang, S. Sudarsky, and G. Lo. On dynamic multi-rigid-body contact problems with coulomb friction. *Zeitschrift für Angewandte Mathematik und Mechanik*, 77(4), pp. 267–280, 1997.
- [39] J. Trinkle, J. Tzitzouris, and J. Pang. Dynamic multi-rigid-systems with concurrent distributed contacts. *The Royal Society Philosophical Transactions: Mathematical, Physical and Engineering Sciences*, 359, pp. 2575–2593, 2001.
- [40] J. Tzitzouris. *Numerical Resolution of Frictional Multi-Rigid-Body Systems via Fully-Implicit Time-Stepping and Nonlinear Complementarity*. PhD thesis, Department of Mathematical Sciences, The Johns Hopkins University, Baltimore, MD, 2001.
- [41] C. Ullrich and D. K. Pai. Contact response maps for real time dynamic simulation. In *Proceedings of the 1998 IEEE International Conference on Robotics and Automation*, pp. 1950–1957, 1998.
- [42] Y. Wang and M. T. Mason. Modeling impact dynamics for robotic operations. In *Proceedings of the 1987 IEEE International Conference on Robotics and Automation*, pp. 678–685, 1987.
- [43] Y.-T. Wang and V. Kumar. Simulation of mechanical systems with unilateral constraints. *Journal of Mechanical Design*, 116(2), pp. 571–580, 1994.
- [44] S. Wu, E. J. Haug, and S. M. Yang. Dynamics of mechanical systems with coulomb friction, stiction, impact and constraint addition-deletion - i-iii. *Mechanism and Machine Theory*, 21(5), pp. 401–425, 1986.

A Influence matrix of stiffness coefficients

The analytical expressions given below pertain to a contact patch and are derived from the classical approach by Boussinesq and Cerruti. See [17, 25] for the details of the derivation. For simplicity, the patch index ν is omitted.

$$K = \begin{pmatrix} K_{nn} & K_{nt} & K_{no} \\ K_{tn} & K_{tt} & K_{to} \\ K_{on} & K_{ot} & K_{oo} \end{pmatrix} = \Xi^{-1} \equiv \begin{pmatrix} \xi_{nn} & \xi_{nt} & \xi_{no} \\ \xi_{tn} & \xi_{tt} & \xi_{to} \\ \xi_{on} & \xi_{ot} & \xi_{oo} \end{pmatrix}^{-1}$$

$$\xi_{nn}(\mathbf{r}_i, \mathbf{r}_j) = \begin{cases} \frac{1-\nu^2}{\pi\|\mathbf{r}_{ij}\|} \varepsilon & i \neq j \\ 0.95 \frac{1-\nu^2}{\pi\rho_0} \varepsilon & i = j \end{cases}$$

$$\xi_{tt}(\mathbf{r}_i, \mathbf{r}_j) = \begin{cases} \frac{1+\nu}{\pi\|\mathbf{r}_{ij}\|} \left(1-\nu + \frac{\langle \mathbf{r}_{ij}, \hat{\mathbf{t}} \rangle^2}{\|\mathbf{r}_{ij}\|^2} \nu\right) \varepsilon & i \neq j \\ \frac{(1+\nu)(2-\nu)}{\sqrt{\pi}\rho_0} \varepsilon & i = j \end{cases}$$

$$\xi_{oo}(\mathbf{r}_i, \mathbf{r}_j) = \begin{cases} \frac{1+\nu}{\pi\|\mathbf{r}_{ij}\|} \left(1-\nu + \frac{\langle \mathbf{r}_{ij}, \hat{\mathbf{o}} \rangle^2}{\|\mathbf{r}_{ij}\|^2} \nu\right) \varepsilon & i \neq j \\ \frac{(1+\nu)(2-\nu)}{\sqrt{\pi}\rho_0} \varepsilon & i = j \end{cases}$$

$$\xi_{nt}(\mathbf{r}_i, \mathbf{r}_j) = \begin{cases} \frac{(1-2\nu)(1+\nu)}{2\pi} \frac{\langle \mathbf{r}_{ij}, \hat{\mathbf{t}} \rangle}{\|\mathbf{r}_{ij}\|^2} \varepsilon & i \neq j \\ 0 & i = j \end{cases}$$

$$\xi_{tn}(\mathbf{r}_i, \mathbf{r}_j) = \begin{cases} -\frac{(1-2\nu)(1+\nu)}{2\pi} \frac{\langle \mathbf{r}_{ij}, \hat{\mathbf{t}} \rangle}{\|\mathbf{r}_{ij}\|^2} \varepsilon & i \neq j \\ 0 & i = j \end{cases}$$

$$\xi_{no}(\mathbf{r}_i, \mathbf{r}_j) = \begin{cases} \frac{(1-2\nu)(1+\nu)}{2\pi} \frac{\langle \mathbf{r}_{ij}, \hat{\mathbf{o}} \rangle}{\|\mathbf{r}_{ij}\|^2} \varepsilon & i \neq j \\ 0 & i = j \end{cases}$$

$$\xi_{on}(\mathbf{r}_i, \mathbf{r}_j) = \begin{cases} -\frac{(1-2\nu)(1+\nu)}{2\pi} \frac{\langle \mathbf{r}_{ij}, \hat{\mathbf{o}} \rangle}{\|\mathbf{r}_{ij}\|^2} \varepsilon & i \neq j \\ 0 & i = j \end{cases}$$

$$\xi_{to}(\mathbf{r}_i, \mathbf{r}_j) = \begin{cases} \frac{(1+\nu)}{\pi} \frac{\langle \mathbf{r}_{ij}, \hat{\mathbf{o}} \rangle \langle \mathbf{r}_{ij}, \hat{\mathbf{t}} \rangle}{\|\mathbf{r}_{ij}\|^3} \varepsilon & i \neq j \\ 0 & i = j \end{cases}$$

$$\xi_{ot}(\mathbf{r}_i, \mathbf{r}_j) = \begin{cases} \frac{(1+\nu)}{\pi} \frac{\langle \mathbf{r}_{ij}, \hat{\mathbf{o}} \rangle \langle \mathbf{r}_{ij}, \hat{\mathbf{t}} \rangle}{\|\mathbf{r}_{ij}\|^3} \varepsilon & i \neq j \\ 0 & i = j \end{cases}$$

where $\mathbf{r}_{ij} \equiv \mathbf{r}_i - \mathbf{r}_j$, \mathbf{r}_i and \mathbf{r}_j are the position vectors of the i th node and j th node in the contact patch respectively. $\hat{\mathbf{t}}$ and $\hat{\mathbf{o}}$ are the unit vectors that span the plane perpendicular to the contact normal. ρ_0 is the characteristic length between two adjacent nodes. ε is the inverse of Young's modulus for the material and ν is the Poisson ratio.

B Proofs of Results

Proof of Proposition 1. The matrix \mathbf{H}^ℓ is the Schur complement of the matrix

$$h^{-1}\mathbf{M}^\ell = h^{-1}M(q^\ell) + \begin{bmatrix} W_n(q^\ell) \\ W_t(q^\ell) \\ W_o(q^\ell) \end{bmatrix}^T \begin{bmatrix} E_{nn} & E_{nt} & E_{no} \\ E_{tn} & E_{tt} & E_{to} \\ E_{on} & E_{ot} & E_{oo} \end{bmatrix} \begin{bmatrix} W_n(q^\ell) \\ W_t(q^\ell) \\ W_o(q^\ell) \end{bmatrix}$$

in

$$\begin{bmatrix} E_{nn} & E_{nt} & E_{no} & \tilde{W}_n(q^\ell) \\ E_{tn} & E_{tt} & E_{to} & \tilde{W}_t(q^\ell) \\ E_{on} & E_{ot} & E_{oo} & \tilde{W}_o(q^\ell) \\ \tilde{W}_n(q^\ell)^T & \tilde{W}_t(q^\ell)^T & \tilde{W}_o(q^\ell)^T & h^{-1}\mathbf{M}^\ell \end{bmatrix} = \begin{bmatrix} E_{nn} & E_{nt} & E_{no} & 0 \\ E_{tn} & E_{tt} & E_{to} & 0 \\ E_{on} & E_{ot} & E_{oo} & 0 \\ 0 & 0 & 0 & \frac{1}{h}M(q^\ell) \end{bmatrix} + \begin{bmatrix} 0 & 0 & 0 \\ 0 & 0 & 0 \\ 0 & 0 & 0 \\ W_n(q^\ell)^T & W_t(q^\ell)^T & W_o(q^\ell)^T \end{bmatrix} \begin{bmatrix} E_{nn} & E_{nt} & E_{no} \\ E_{tn} & E_{tt} & E_{to} \\ E_{on} & E_{ot} & E_{oo} \end{bmatrix} \begin{bmatrix} 0 & 0 & 0 & W_n(q^\ell) \\ 0 & 0 & 0 & W_t(q^\ell) \\ 0 & 0 & 0 & W_o(q^\ell) \end{bmatrix},$$

which is symmetric positive definite. Consequently, so is \mathbf{H}^ℓ . \square

Proof of Theorem 2. The proof of part (a) is already sketched in Section 4. That of part (b) follows from the fact that for each ℓ , the problem (13) has a unique solution when the friction coefficients are sufficiently small [38]. Since there are only N such problems, one for each time step, part (b) follows readily. \square

Proof of Theorem 3. The matrix $\tilde{\mathbf{J}}^\ell$ is copositive on the nonnegative orthant $\mathfrak{R}_+^{5n_s^2 n_c}$. Thus

the theorem holds if we demonstrate that

$$\begin{array}{r}
0 \leq \left(\begin{array}{c} \lambda_n^{\ell+1} \\ u_t^{\ell+1} \\ v_t^{\ell+1} \\ u_o^{\ell+1} \\ v_o^{\ell+1} \end{array} \right) \perp \left(\begin{array}{c} \lambda_n^{\ell+1} \\ u_t^{\ell+1} \\ v_t^{\ell+1} \\ u_o^{\ell+1} \\ v_o^{\ell+1} \end{array} \right) \geq 0 \\
0 \leq \left(\begin{array}{c} \lambda_n^{\ell+1} \\ u_t^{\ell+1} \\ v_t^{\ell+1} \\ u_o^{\ell+1} \\ v_o^{\ell+1} \end{array} \right) \perp \tilde{\mathbf{J}}^\ell \left(\begin{array}{c} \lambda_n^{\ell+1} \\ u_t^{\ell+1} \\ v_t^{\ell+1} \\ u_o^{\ell+1} \\ v_o^{\ell+1} \end{array} \right) \geq 0 \\
0 \leq \left(\begin{array}{c} \lambda_n^{\ell+1} \\ u_t^{\ell+1} \\ v_t^{\ell+1} \\ u_o^{\ell+1} \\ v_o^{\ell+1} \end{array} \right) \perp \left(\begin{array}{c} \lambda_n^{\ell+1} \\ u_t^{\ell+1} \\ v_t^{\ell+1} \\ u_o^{\ell+1} \\ v_o^{\ell+1} \end{array} \right) \geq 0 \\
0 \leq \left(\begin{array}{c} \lambda_n^{\ell+1} \\ u_t^{\ell+1} \\ v_t^{\ell+1} \\ u_o^{\ell+1} \\ v_o^{\ell+1} \end{array} \right) \perp \left(\begin{array}{c} \lambda_n^{\ell+1} \\ u_t^{\ell+1} \\ v_t^{\ell+1} \\ u_o^{\ell+1} \\ v_o^{\ell+1} \end{array} \right) \geq 0 \\
0 \leq \left(\begin{array}{c} \lambda_n^{\ell+1} \\ u_t^{\ell+1} \\ v_t^{\ell+1} \\ u_o^{\ell+1} \\ v_o^{\ell+1} \end{array} \right) \perp \left(\begin{array}{c} \lambda_n^{\ell+1} \\ u_t^{\ell+1} \\ v_t^{\ell+1} \\ u_o^{\ell+1} \\ v_o^{\ell+1} \end{array} \right) \geq 0
\end{array}
\Rightarrow \begin{pmatrix} \tilde{b}_n^\ell \\ \tilde{b}_t^\ell \\ -\tilde{b}_t^\ell \\ \tilde{b}_o^\ell \\ -\tilde{b}_o^\ell \end{pmatrix}^T \begin{pmatrix} \lambda_n^{\ell+1} \\ u_t^{\ell+1} \\ v_t^{\ell+1} \\ u_o^{\ell+1} \\ v_o^{\ell+1} \end{pmatrix} \geq 0.$$

By the structure of $\tilde{\mathbf{J}}^\ell$, if the left-hand side holds, then we must have $\lambda_n^{\ell+1} = 0$ and

$$u_t^{\ell+1} - v_t^{\ell+1} = u_o^{\ell+1} - v_o^{\ell+1} = 0.$$

This clearly implies that the right-hand side, hence, the desired implication, holds. \square

Proof of Theorem 4. It suffices to identify the set Ω such that the problem (13) has finitely many solutions for every $\mu \notin \Omega$. We rely on the equivalent LCP (18) to accomplish this task. Let $(\lambda_n^{\ell+1}, u_{t,o}^{\ell+1}, v_{t,o}^{\ell+1})$ be an arbitrary tuple of solution to (18). Let

$$\begin{aligned}
\alpha_n &\equiv \{i : \lambda_n^{\ell+1} > 0\}, \\
\alpha_t &\equiv \{i : u_{it}^{\ell+1} \text{ or } v_{it}^{\ell+1} > 0\}, \\
\alpha_o &\equiv \{i : u_{io}^{\ell+1} \text{ or } v_{io}^{\ell+1} > 0\}
\end{aligned}$$

be the supports of the respective variables. Recalling the variables $s_{it,o}^{\ell+1} = u_{it,o}^{\ell+1} - v_{it,o}^{\ell+1}$, we see that

$$\mathbf{x}_\alpha \equiv \left\{ \left(\lambda_{in}^{\ell+1} \right)_{i \in \alpha_n}, \left(s_{it}^{\ell+1} \right)_{i \in \alpha_t}, \left(s_{io}^{\ell+1} \right)_{i \in \alpha_o} \right\}$$

must satisfy a system of linear equations of the form:

$$\mathbf{b}_\alpha + \mathbf{M}_{\alpha\alpha}(\mu)\mathbf{x}_\alpha = 0$$

where $\mathbf{M}_{\alpha\alpha}(\mu)$ is the sum of a positive definite matrix (an appropriate submatrix of $\tilde{\mathbf{J}}_1^\ell$), which is independent of μ , and a simple matrix (an appropriate submatrix of $\tilde{\mathbf{J}}_2^\ell$), which depends on μ_i for $i \in \alpha_n$. As such, $\mathbf{M}_{\alpha\alpha}(\mu)$ is nonsingular for all but finitely many μ . Since there is only a finite number of different index sets α , it follows that for each μ not in a finite set Ω (where $\mathbf{M}_{\alpha\alpha}(\mu)$ is singular), there can only be a finite number of $\lambda_n^{\ell+1}$ and of induced $s_{t,o}^{\ell+1}$ that satisfy the LCP (18). (Note: we make no claim about the finiteness of the auxiliary u and v variables.) Hence the number of $s_n^{\ell+1}$ is also finite for each $\mu \notin \Omega$. Since these variables $\lambda_n^{\ell+1}$ and $s_{n,t,o}^{\ell+1}$ completely determine the solution trajectories of the compliant contact model, it follows that there are only finitely many such trajectories for each $\mu \notin \Omega$. \square

Proof of Lemma 5. We proceed by induction on ℓ . Suppose that the assertions are valid for $\ell \geq 0$. The induction hypothesis on (b) implies (19) at step ℓ . On the one hand, we have

$$\begin{aligned}
& (\nu^{\ell+1,\varepsilon})^T M(q^{\ell,\varepsilon}) \nu^{\ell+1,\varepsilon} - (\nu^{\ell+1,\varepsilon})^T [M(q^{\ell,\varepsilon}) \nu^{\ell,\varepsilon} + h f(t_\ell, q^{\ell,\varepsilon}, \nu^{\ell,\varepsilon})] \\
&= \left[\nu^{\ell+1,\varepsilon} - \frac{1}{2} \nu^{\ell,\varepsilon} - \frac{1}{2h} f(t_\ell, q^{\ell,\varepsilon}, \nu^{\ell,\varepsilon}) \right]^T M(q^{\ell,\varepsilon}) \left[\nu^{\ell+1,\varepsilon} - \frac{1}{2} \nu^{\ell,\varepsilon} - \frac{1}{2h} f(t_\ell, q^{\ell,\varepsilon}, \nu^{\ell,\varepsilon}) \right] \\
&\quad - \frac{1}{4} \left[\nu^{\ell,\varepsilon} - \frac{1}{h} f(t_\ell, q^{\ell,\varepsilon}, \nu^{\ell,\varepsilon}) \right]^T M(q^{\ell,\varepsilon}) \left[\nu^{\ell,\varepsilon} - \frac{1}{h} f(t_\ell, q^{\ell,\varepsilon}, \nu^{\ell,\varepsilon}) \right] \\
&\geq -\frac{1}{4} \left[\nu^{\ell,\varepsilon} - \frac{1}{h} f(t_\ell, q^{\ell,\varepsilon}, \nu^{\ell,\varepsilon}) \right]^T M(q^{\ell,\varepsilon}) \left[\nu^{\ell,\varepsilon} - \frac{1}{h} f(t_\ell, q^{\ell,\varepsilon}, \nu^{\ell,\varepsilon}) \right];
\end{aligned}$$

on the other hand, premultiplying (11) by $(\nu^{\ell+1,\varepsilon})^T$, we obtain

$$\begin{aligned}
& (\nu^{\ell+1,\varepsilon})^T M(q^{\ell,\varepsilon}) \nu^{\ell+1,\varepsilon} - (\nu^{\ell+1,\varepsilon})^T [M(q^{\ell,\varepsilon}) \nu^{\ell,\varepsilon} + h f(t_\ell, q^{\ell,\varepsilon}, \nu^{\ell,\varepsilon})] \\
&= h \begin{bmatrix} W_n(q^{\ell,\varepsilon}) \nu^{\ell+1,\varepsilon} \\ W_t(q^{\ell,\varepsilon}) \nu^{\ell+1,\varepsilon} \\ W_o(q^{\ell,\varepsilon}) \nu^{\ell+1,\varepsilon} \end{bmatrix}^T \begin{pmatrix} \lambda_n^{\ell+1,\varepsilon} \\ \lambda_t^{\ell+1,\varepsilon} \\ \lambda_o^{\ell+1,\varepsilon} \end{pmatrix} \\
&= h \begin{bmatrix} W_n(q^{\ell,\varepsilon}) \nu^{\ell+1,\varepsilon} - s_n^{\ell+1,\varepsilon} \\ W_t(q^{\ell,\varepsilon}) \nu^{\ell+1,\varepsilon} - s_t^{\ell+1,\varepsilon} \\ W_o(q^{\ell,\varepsilon}) \nu^{\ell+1,\varepsilon} - s_o^{\ell+1,\varepsilon} \end{bmatrix}^T \begin{pmatrix} \lambda_n^{\ell+1,\varepsilon} \\ \lambda_t^{\ell+1,\varepsilon} \\ \lambda_o^{\ell+1,\varepsilon} \end{pmatrix} + h \begin{bmatrix} s_n^{\ell+1,\varepsilon} \\ s_t^{\ell+1,\varepsilon} \\ s_o^{\ell+1,\varepsilon} \end{bmatrix}^T \begin{pmatrix} \lambda_n^{\ell+1,\varepsilon} \\ \lambda_t^{\ell+1,\varepsilon} \\ \lambda_o^{\ell+1,\varepsilon} \end{pmatrix} \\
&\leq h \begin{bmatrix} W_n(q^{\ell,\varepsilon}) \nu^{\ell+1,\varepsilon} - s_n^{\ell+1,\varepsilon} \\ W_t(q^{\ell,\varepsilon}) \nu^{\ell+1,\varepsilon} - s_t^{\ell+1,\varepsilon} \\ W_o(q^{\ell,\varepsilon}) \nu^{\ell+1,\varepsilon} - s_o^{\ell+1,\varepsilon} \end{bmatrix}^T \begin{pmatrix} \lambda_n^{\ell+1,\varepsilon} \\ \lambda_t^{\ell+1,\varepsilon} \\ \lambda_o^{\ell+1,\varepsilon} \end{pmatrix} \\
&= h \begin{pmatrix} W_n(q^{\ell,\varepsilon}) \nu^{\ell+1,\varepsilon} - s_n^{\ell+1,\varepsilon} \\ W_t(q^{\ell,\varepsilon}) \nu^{\ell+1,\varepsilon} - s_t^{\ell+1,\varepsilon} \\ W_o(q^{\ell,\varepsilon}) \nu^{\ell+1,\varepsilon} - s_o^{\ell+1,\varepsilon} \end{pmatrix}^T \left\{ \begin{bmatrix} K_{nn} & K_{nt} & K_{no} \\ K_{tn} & K_{tt} & K_{to} \\ K_{on} & K_{ot} & K_{oo} \end{bmatrix} \begin{pmatrix} \delta_n^{\ell,\varepsilon} \\ \delta_t^{\ell,\varepsilon} \\ \delta_o^{\ell,\varepsilon} \end{pmatrix} + \right. \\
&\quad \left. \begin{bmatrix} E_{nn} & E_{nt} & E_{no} \\ E_{tn} & E_{tt} & E_{to} \\ E_{on} & E_{ot} & E_{oo} \end{bmatrix} \begin{pmatrix} s_n^{\ell+1,\varepsilon} - W_n(q^{\ell,\varepsilon}) \nu^{\ell+1,\varepsilon} \\ s_t^{\ell+1,\varepsilon} - W_t(q^{\ell,\varepsilon}) \nu^{\ell+1,\varepsilon} \\ s_o^{\ell+1,\varepsilon} - W_o(q^{\ell,\varepsilon}) \nu^{\ell+1,\varepsilon} \end{pmatrix} \right\}.
\end{aligned}$$

Consequently, we deduce

$$\begin{aligned}
& \begin{pmatrix} \frac{1}{\sqrt{\varepsilon}} \left(s_n^{\ell+1,\varepsilon} - W_n(q^{\ell,\varepsilon})\nu^{\ell+1,\varepsilon} \right) \\ \frac{1}{\sqrt{\varepsilon}} \left(s_t^{\ell+1,\varepsilon} - W_t(q^{\ell,\varepsilon})\nu^{\ell+1,\varepsilon} \right) \\ \frac{1}{\sqrt{\varepsilon}} \left(s_o^{\ell+1,\varepsilon} - W_o(q^{\ell,\varepsilon})\nu^{\ell+1,\varepsilon} \right) \end{pmatrix}^T \left\{ \varepsilon \begin{bmatrix} K_{nn} & K_{nt} & K_{no} \\ K_{tn} & K_{tt} & K_{to} \\ K_{on} & K_{ot} & K_{oo} \end{bmatrix} \begin{pmatrix} \frac{1}{\sqrt{\varepsilon}} \delta_n^{\ell,\varepsilon} \\ \frac{1}{\sqrt{\varepsilon}} \delta_t^{\ell,\varepsilon} \\ \frac{1}{\sqrt{\varepsilon}} \delta_o^{\ell,\varepsilon} \end{pmatrix} \right\} + \\
& \varepsilon \begin{bmatrix} E_{nn} & E_{nt} & E_{no} \\ E_{tn} & E_{tt} & E_{to} \\ E_{on} & E_{ot} & E_{oo} \end{bmatrix} \begin{pmatrix} \frac{1}{\sqrt{\varepsilon}} \left(s_n^{\ell+1,\varepsilon} - W_n(q^{\ell,\varepsilon})\nu^{\ell+1,\varepsilon} \right) \\ \frac{1}{\sqrt{\varepsilon}} \left(s_t^{\ell+1,\varepsilon} - W_t(q^{\ell,\varepsilon})\nu^{\ell+1,\varepsilon} \right) \\ \frac{1}{\sqrt{\varepsilon}} \left(s_o^{\ell+1,\varepsilon} - W_o(q^{\ell,\varepsilon})\nu^{\ell+1,\varepsilon} \right) \end{pmatrix} \\
& \leq \frac{1}{4} \left[\nu^{\ell,\varepsilon} - \frac{1}{h} f(t_\ell, q^{\ell,\varepsilon}, \nu^{\ell,\varepsilon}) \right]^T M(q^{\ell,\varepsilon}) \left[\nu^{\ell,\varepsilon} - \frac{1}{h} f(t_\ell, q^{\ell,\varepsilon}, \nu^{\ell,\varepsilon}) \right]
\end{aligned}$$

By (A1), assertion (a) holds. This implies

$$\lim_{\varepsilon \downarrow 0} \left[s_{n,t,o}^{\ell+1,\varepsilon} - W_{n,t,o}(q^{\ell,\varepsilon})\nu^{\ell+1,\varepsilon} \right] = 0.$$

Thus (b) follows readily from (9) and the induction hypothesis. From the above derivation, we have

$$\begin{aligned}
& (\nu^{\ell+1,\varepsilon})^T M(q^{\ell,\varepsilon}) \nu^{\ell+1,\varepsilon} - (\nu^{\ell+1,\varepsilon})^T \left[M(q^{\ell,\varepsilon})\nu^{\ell,\varepsilon} + h f(t_\ell, q^{\ell,\varepsilon}, \nu^{\ell,\varepsilon}) \right] \\
& \leq \begin{pmatrix} \frac{1}{\sqrt{\varepsilon}} \left(s_n^{\ell+1,\varepsilon} - W_n(q^{\ell,\varepsilon})\nu^{\ell+1,\varepsilon} \right) \\ \frac{1}{\sqrt{\varepsilon}} \left(s_t^{\ell+1,\varepsilon} - W_t(q^{\ell,\varepsilon})\nu^{\ell+1,\varepsilon} \right) \\ \frac{1}{\sqrt{\varepsilon}} \left(s_o^{\ell+1,\varepsilon} - W_o(q^{\ell,\varepsilon})\nu^{\ell+1,\varepsilon} \right) \end{pmatrix}^T \left\{ \varepsilon \begin{bmatrix} K_{nn} & K_{nt} & K_{no} \\ K_{tn} & K_{tt} & K_{to} \\ K_{on} & K_{ot} & K_{oo} \end{bmatrix} \begin{pmatrix} \frac{1}{\sqrt{\varepsilon}} \delta_n^{\ell,\varepsilon} \\ \frac{1}{\sqrt{\varepsilon}} \delta_t^{\ell,\varepsilon} \\ \frac{1}{\sqrt{\varepsilon}} \delta_o^{\ell,\varepsilon} \end{pmatrix} \right\},
\end{aligned}$$

which easily yields (c). Finally, (d) follows from (11) and the boundedness of $\nu^{\ell+1,\varepsilon}$ and $(q^{\ell,\varepsilon}, \nu^{\ell,\varepsilon})$. \square

Proof of Theorem 6. Assume for the sake of contradiction that for some ℓ , the sequence

$$\left\{ \left(\lambda_n^{\ell+1,\varepsilon_k}, \lambda_t^{\ell+1,\varepsilon_k}, \lambda_o^{\ell+1,\varepsilon_k} \right) \right\}$$

is unbounded as $k \rightarrow \infty$. We can then further assume, without loss of generality, that

$$\lim_{k \rightarrow \infty} \left\| \left(\lambda_n^{\ell+1,\varepsilon_k}, \lambda_t^{\ell+1,\varepsilon_k}, \lambda_o^{\ell+1,\varepsilon_k} \right) \right\| = \infty$$

and

$$\lim_{k \rightarrow \infty} \frac{\left(\lambda_n^{\ell+1, \varepsilon_k}, \lambda_t^{\ell+1, \varepsilon_k}, \lambda_o^{\ell+1, \varepsilon_k} \right)}{\left\| \left(\lambda_n^{\ell+1, \varepsilon_k}, \lambda_t^{\ell+1, \varepsilon_k}, \lambda_o^{\ell+1, \varepsilon_k} \right) \right\|} = \left(\lambda_n^{\ell+1, *}, \lambda_t^{\ell+1, *}, \lambda_o^{\ell+1, *} \right)$$

for some nonzero tuple $\lambda_{n,t,o}^{\ell+1, *}$. Since

$$\limsup_{k \rightarrow \infty} \left\| W_n(q^{\ell, \varepsilon_k})^T \lambda_n^{\ell+1, \varepsilon_k} + W_t(q^{\ell, \varepsilon_k})^T \lambda_t^{\ell+1, \varepsilon_k} + W_o(q^{\ell, \varepsilon_k})^T \lambda_o^{\ell+1, \varepsilon_k} \right\| < \infty,$$

it is easy to show, by a straightforward limiting argument, that $\lambda_{n,t,o}^{\ell+1, *}$ satisfies the left-hand conditions in the implication (20). But this is a contradiction because this tuple is nonzero. Consequently, the boundedness of the forces follows. The last assertion about the limiting tuple $(q^{\ell+1, \infty}, \nu^{\ell+1, \infty}, \lambda_{n,t,o}^{\ell+1, \infty})$ can be proved by a similar limit argument. \square